

AD-A067 977

HYDROTRONICS INC SAN DIEGO CA

F/6 9/3

EXPERIMENTAL PERFORMANCE MEASUREMENTS OF ADAPTIVE NOISE CANCELL--ETC (U)

SEP 78 R H HEARN, M SHENSA, M WHALEY

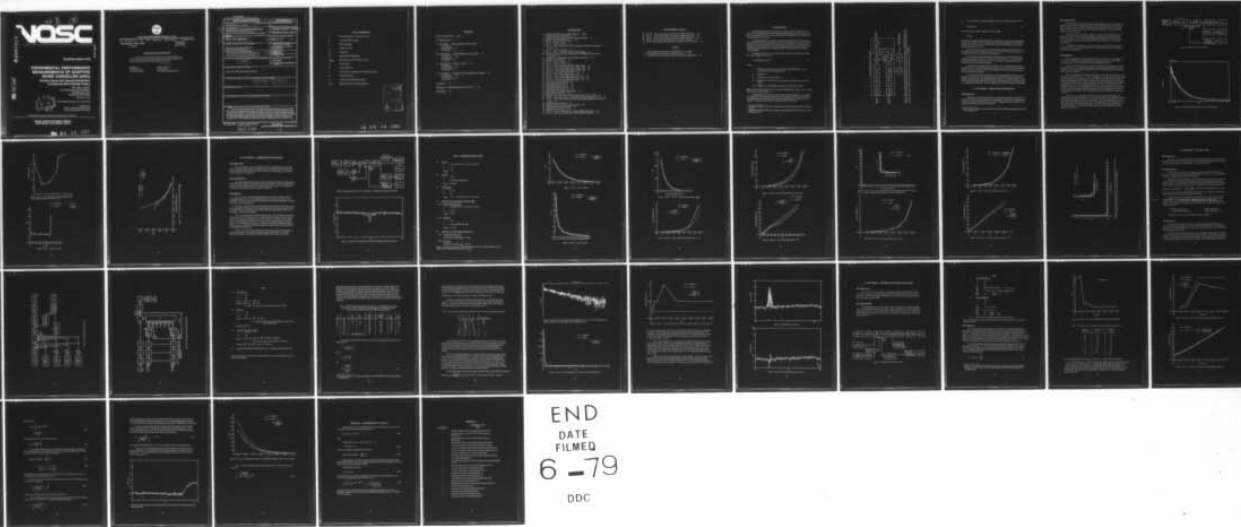
N00123-76-C-1937

UNCLASSIFIED

NOSC-TR-372

NL

OF  
AD  
A067 977



AD A067977

**NOSC**

NOSC TR 372

Technical Report 372

**EXPERIMENTAL PERFORMANCE  
MEASUREMENTS OF ADAPTIVE  
NOISE CANCELLER (ANC)**

**Various Inputs and Internal Parameters  
Correspond with Existing Theory**

RH Hearn, NOSC,  
and M Shensa and M Whaley,  
Hydrotronics, Inc.  
(NOO123-76-C-1937)

September 1978

Final Report: October 1977-June 1978

Prepared for  
Chief of Naval Operations and  
Naval Sea Systems Command



APPROVED FOR PUBLIC RELEASE; DISTRIBUTION UNLIMITED

**NAVAL OCEAN SYSTEMS CENTER  
SAN DIEGO, CALIFORNIA 92152**

29 04 24 062

DDC FILE COPY,



NAVAL OCEAN SYSTEMS CENTER, SAN DIEGO, CA 92152

---

AN ACTIVITY OF THE NAVAL MATERIAL COMMAND

RR GAVAZZI, CAPT USN

Commander

HL BLOOD

Technical Director

#### ADMINISTRATIVE INFORMATION

The work reported herein was sponsored by CNO (OP 009G) and NAVSEA (661C). It was performed by Naval Ocean Systems Center and under contract N00123-76-C-1937 by Hydrotronics, Inc.

Released by  
RH Hearn, Head  
Electronics Division

Under authority of  
DA Kunz, Head  
Fleet Engineering Department

UNCLASSIFIED

SECURITY CLASSIFICATION OF THIS PAGE (When Data Entered)

REPORT DOCUMENTATION PAGE		READ INSTRUCTIONS BEFORE COMPLETING FORM
1. REPORT NUMBER NOSC Technical Report 372 (TR372)	2. GOVT ACCESSION NO.	3. RECIPIENT'S CATALOG NUMBER (9)
4. TITLE (and Subtitle) EXPERIMENTAL PERFORMANCE MEASUREMENTS OF ADAPTIVE NOISE CANCELLER (ANC). Various Inputs and Internal Parameters Correspond with Existing Theory.	5. TYPE OF REPORT & PERIOD COVERED Final Report October 1977 - June 1978	
6. AUTHOR(s) RH Hearn, M Shensa, and M Whaley	7. PERFORMING ORG. REPORT NUMBER	
8. CONTRACT OR GRANT NUMBER(s) N00123-76-C-1937	9. PERFORMING ORGANIZATION NAME AND ADDRESS Naval Ocean Systems Center, San Diego, CA Hydrotronics, Inc., San Diego, CA	
10. PROGRAM ELEMENT, PROJECT, TASK AREA & WORK UNIT NUMBERS 31015N, SS06638A; and 63553N, 20979, 632 WS16	11. CONTROLLING OFFICE NAME AND ADDRESS Chief of Naval Operations (OP 009G), Washington, D.C. Naval Sea Systems Command (661C), Washington, D.C.	
12. REPORT DATE September 1978	13. NUMBER OF PAGES 44	
14. MONITORING AGENCY NAME & ADDRESS (if different from Controlling Office) (12) 47p.	15. SECURITY CLASS. (of this report) UNCLASSIFIED	
15a. DECLASSIFICATION/DOWNGRADING SCHEDULE		
16. DISTRIBUTION STATEMENT (of this Report) Approved for public release; distribution unlimited		
17. DISTRIBUTION STATEMENT (of the abstract entered in Block 20, if different from Report) (18) NOSC (19) TR-372		
18. SUPPLEMENTARY NOTES		
19. KEY WORDS (Continue on reverse side if necessary and identify by block number)		
20. ABSTRACT (Continue on reverse side if necessary and identify by block number) This report describes tests performed on the Adaptive Noise Canceller (ANC) as part of a joint NUSC/ NOSC program investigating adaptive processors. The purpose of the test was to evaluate the effects of various inputs and internal parameters on the operating characteristics of the ANC. The primary dependent parameters of interest were the adaptive time constant, the notch width, and notch depth. These were measured as functions of the filter length, feedback constant, reference power spectrum and delay. The number of reference inputs was varied as well. The experimental results are plotted and show excellent agreement with existing theory.		

DD FORM 1 JAN 73 1473

EDITION OF 1 NOV 65 IS OBSOLETE  
S/N 0102-LF-014-6601

UNCLASSIFIED

SECURITY CLASSIFICATION OF THIS PAGE (When Data Entered)

411 130

LB



# LIST OF PARAMETERS

$\mu$	Feedback constant — front panel setting
$\hat{\mu}$	Internal feedback constant
N	ANC filter length
$f_s$	Sample rate in Hz
$\sigma_n^2$	Noise power
$\sigma_s^2$	Signal (sinusoid) RMS power
$V_{RMS}$	Mean square power of reference in volts
$\Delta_p$	Primary delay
W	Notch width in Hz
$\tau$	Time constant of adaptive noise canceller in seconds
D	Notch depth in dB
$\Delta f$	Frequency separation (Hz) of signals
SNR	Signal-to-noise ratio in dB (total power)

APPROVAL FOR	
NTIS	Write Section <input checked="" type="checkbox"/>
DDC	Dist. Section <input type="checkbox"/>
DDC - REPRODUCED	<input type="checkbox"/>
JUSTIFICATION	
BY	
DISTRIBUTION/AVAILABILITY CODES	
Dist.	AVAIL. AND/OR SPECIAL
A	

## CONTENTS

LIST OF PARAMETERS . . . page 1

I. INTRODUCTION . . . 5

II. TEST SERIES 1 – BROADBAND CANCELLATION . . . 7

Test Objective . . . 7

Test Description . . . 8

Test Results . . . 8

III. TEST SERIES 2 – NARROWBAND CANCELLATION . . . 14

Test Objective . . . 14

Test Description . . . 14

Test Results . . . 14

IV. TEST SERIES 3 – MULTIPLE LINES . . . 23

Test Objective . . . 23

Test Description . . . 23

Test Results . . . 23

V. TEST SERIES 4 – REFERENCE CONTAMINATED BY NOISE . . . 34

Test Objective . . . 34

Test Description . . . 34

Test Results . . . 35

APPENDIX A . . . 39

APPENDIX B – MEASUREMENT OF  $\tau$  IN TEST 3.1 . . . 43

APPENDIX C . . . 44

## ILLUSTRATIONS

- 1 Diagram of adaptive noise canceller (ANC) box . . . page 6
- 2 Experimental setup for Test Series 1 . . . 9
- 3 Example of the determination of  $\tau$  from the output voltage . . . 9
- 4 Outline of parameters for test series 1 . . . 10
- 5 Test 1.1 – plot of  $\tau$  versus  $\mu$  . . . 11
- 6 Test 1.2 – plot of  $\tau$  versus  $N$  . . . 11
- 7 Test 1.3 – plot of ANC transfer function magnitude at 500 Hz versus delay for  $N = 64$  . . . 12
- 8 Test 1.3 – plot of  $\tau$  versus  $\Delta p$  . . . 12
- 9 Test 1.4 – plot of  $\tau$  versus the reference voltage,  $V_{RMS}$  . . . 13
- 10 Experimental setup for test 2.1 through test 2.5 the signal was a sine wave at 224.75 Hz . . . 15
- 11 Example of the measurement of notch width for test series 2 . . . 15
- 12 Parameters for test series 2 . . . 16
- 13 Test 2.1 – plot of  $\tau$  versus  $\mu$  . . . 17
- 14 Test 2.2 – plot of  $\tau$  versus  $\mu$  . . . 17
- 15 Test 2.3 – plot of  $\tau$  versus the reference voltage,  $V_{RMS}$  . . . 18
- 16 Test 2.4.1 – plot of notch width versus  $\mu$  with  $N = 32$  . . . 18
- 17 Test 2.4.1 – plot of notch width versus  $\mu$  with  $N = 512$  . . . 19
- 18 Test 2.4.2 – notch width versus  $N$  with  $\mu = 2^{-8}$  . . . 19
- 19 Test 2.4 – plot of notch width versus  $\tau$  . . . 20
- 20 Test 2.5.1 – plot of notch width versus  $\mu$  for  $N = 32$  . . . 20
- 21 Test 2.5.1 – plot of notch width versus  $\mu$  for  $N = 512$  . . . 21
- 22 Test 2.5.2 – plot of notch width versus  $N$  for  $\mu = 2^{-8}$  . . . 21
- 23 Test 2.5 plot of notch width versus  $\tau$  . . . 22
- 24 Experimental setup for test 3.1 . . . 24
- 25 Experimental setup for test 3.2 . . . 24
- 26 Experimental setup for test 3.3 . . . 25
- 27 Experimental setup for test 3.4 . . . 26
- 28 Block diagram of multiple reference ANC . . . 27
- 29 Parameters for test series 3 . . . 28
- 30 Example of the noise canceller output voltage in test 3.1 for  $\Delta f = 2$  Hz . . . 31
- 31 Test 3.1 – plot of decay time,  $\tau$ , as a function of frequency separation of  $\Delta f$  . . . 31
- 32 Test 3.2 – plot of notch width as a function of frequency separation in the primary input . . . 32
- 33 Output spectrum for test 3.4 . . . 33
- 34 Spectrum of noise canceller output for test 3.4 . . . 34
- 35 Experimental setup for test series 4 . . . 35
- 36 Parameters for test series 4 . . . 35
- 37 Test 4.1 – plot of  $\tau$  versus SNR, the reference signal-to-noise ratio . . . 36
- 38 Test 4.2 – plot of notch width versus reference signal-to-noise ratio . . . 37

### ILLUSTRATIONS (continued)

- 39 Test 4.2 – plot of notch depth versus reference signal-to-noise ratio . . . 37
- 40 Test 4.3 – plot of notch width versus reference signal-to-noise ratio . . . 38
- 41 Test 4.3 – plot of notch depth versus reference signal-to-noise ratio . . . 38
- A-1 Output of ANC with no post-filter after about 10 time constants . . . 41
- A-2 Test 4.1 with prefilter and post-filter set at 1000 Hz – Plot of  $\tau$  versus  $\mu$  . . . 42

### TABLES

- 1 Notch widths and notch depths for Experiment 3.1 . . . page 29
- 2 Time constants versus frequency separation for Test 3.1 . . . 30
- 3  $\tau$  vs SNR for Test 4.1 compared to values computed by equation (A-8) . . . 36



## I. INTRODUCTION

This report describes tests performed on the Adaptive Noise Canceller (ANC) as part of a joint NUSC/NOSC program investigating adaptive processors. The purpose of the test was to evaluate the effects of various inputs and internal parameters on the operating characteristics of the ANC (fig 1).

The primary dependent parameters of interest were the adaptive time constant  $\tau$ , the notch width  $W$ , and the notch depth  $D$ . These were measured as a function of the feedback constant  $\hat{\mu}$ , the filter length  $N$ , the sample rate  $f_s$ , the reference power  $V_{RMS}$ , and the delay  $\Delta$ . In one experiment, the reference signal-to-noise ratio was varied as well. The testing also included measurement of the ANC transfer function and the input-output cross-correlation.

According to theory (ref 1), the shortest time constant of the ANC for cancelling sine waves in white noise is given by

$$\tau = [2\hat{\mu} (\frac{N}{2} \sigma_s^2 + \sigma_n^2) f_s]^{-1}; \quad (1)$$

where,

$\tau$  = Decay time constant (sec) for the output in volts RMS (this is twice the decay time for the output power),

$f_s$  = Sample rate,

$\hat{\mu}$  = Feedback constant in (Volts)<sup>-2</sup>,

$\sigma_s^2$  = RMS power in (Volts)<sup>2</sup> for the narrowband components in the reference input,

$\sigma_n^2$  = RMS power of the broadband component of the reference input.

Special caution must be taken to be sure that the bandwidth of the "white" noise is exactly Nyquist; i.e.,  $f_s/2$  (see appendix A).

It should also be noted that the above theory assumes convergence of the weights to a linear filter. For a sinusoidal input this is not always the case (ref 2); the solution for the weights may not be stationary and one might even question the definition of "convergence." However, such problems are beyond the scope of this study.

1. Treichler JR, The Spectral Line Enhance, Ph.D Dissertation, Stanford University, Stanford, California, May 1977
2. (NOSC) NUC TN 1617, Adaptive Noise Cancelling of Sinusoidal Interference (U), by J Glover, Unclassified, December 1975

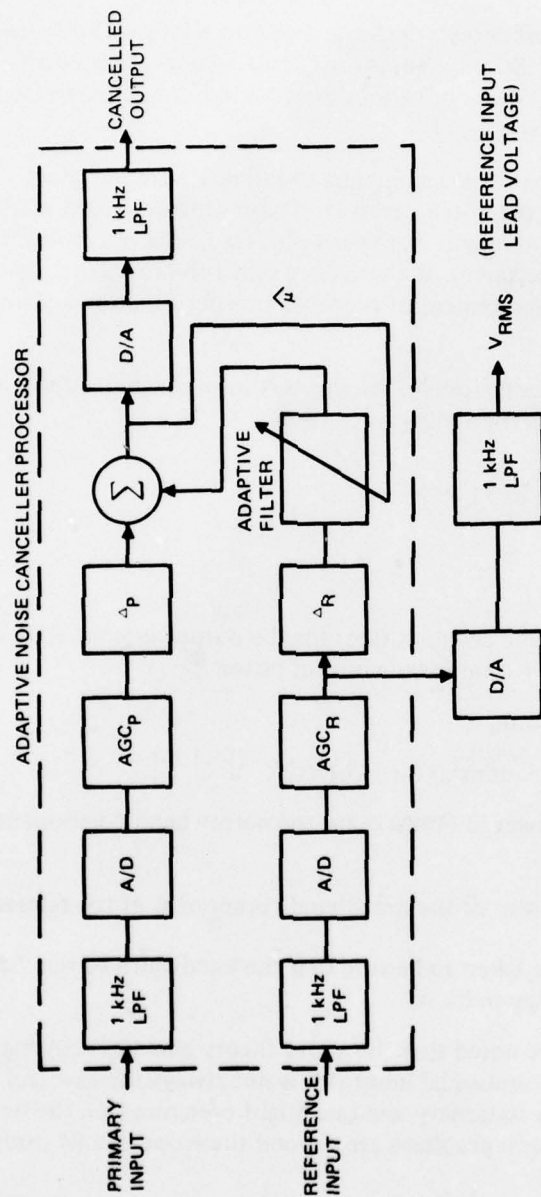


Figure 1. Diagram of Adaptive Noise Canceller (ANC) box. The delay  $\Delta_R$  was fixed at 0. The A/D of the reference was frozen at a gain of 1 in those experiments requiring a variable reference power  $V_{RMS}$ . Internal scaling including the A/O resulted in the relation  $\mu = 2\hat{\mu}$  where  $\mu$  is the front panel setting and  $\hat{\mu}$  is in units of  $(\frac{\text{volt}}{5})^{-2}$ .

For a narrowband reference signal ( $\sigma_s^2 = 0$ ), the notch width  $W$ , is given (ref 2) by

$$W = \hat{\mu} N \sigma_s^2 / \pi, \quad (2)$$

where  $N$  is the filter length. Equations (1) and (2) imply

$$W = \frac{1}{\pi \tau}. \quad (3)$$

The input to the primary and hence the delay, should have no effect on  $\tau$  for narrowband signals (ref 2). However, in the broadband case, the finite filter length must be taken into account (ref 3). In fact, for  $\Delta_p > N$  there will be almost no cancellation. The optimal value of  $\Delta_p$  is about  $N/2$  (ref 3).

Four tests were performed. The first examined broadband cancellation ( $\sigma_s^2 = 0$ ). The time constant  $\tau$  was measured as a function of  $\mu$  (test 1.1),  $N$  (test 1.2),  $\Delta_p$  (test 1.3), and  $\sigma_n^2$  (test 1.4) and then compared with equation (1).

The second test created narrowband cancellation ( $\sigma_n^2 = 0$ ), measuring the time constant as a function of  $\mu$  (test 2.1),  $N$  (test 2.2), and  $\sigma_s^2$  (test 2.3). The notch widths were also measured as a function of  $\mu$  and  $N$  in experiments 2.4 (signal plus noise in primary) and 2.5 (noise alone in primary).

In the third test, multiple lines were present. Test 3.1 contained two sinusoids in the reference; test 3.2 had two sinusoids in the primary; and, test 3.3 had four sinusoids in both the primary and reference. Test 3.4 was similar to 3.3; however, the sinusoids were input to four distinct references.

Test Series 4 investigated the effects of adding an independent noise source to the reference. The first test, 4.1, measured the time constant for a reference consisting of a sinusoid plus white noise. The reference signal-to-noise ratio was varied from  $\infty$  to  $-18$  dB. Test 4.2 measured notch width and notch depth as a function of reference SNR with both signal and noise in the primary. Test 4.3 repeated test 4.2 with noise alone in the primary.

## II. TEST SERIES 1 – BROADBAND CANCELLATION

### TEST OBJECTIVE

The purpose of this series of tests was to examine the performance of the ANC for primary and reference inputs of identical broadband noise. In particular, the adaptive time constant was measured as a function of  $\mu$ ,  $N$ ,  $\Delta_p$ , and  $V_{RMS}$ ; and then compared to that predicted by theory (equations (1) and (A-10)).

3. Widrow B, Glover J, McCool J, et al, Adaptive Noise Cancelling: Principles and Applications, Proc IEEE, vol 63, December 1975

## TEST DESCRIPTION

The experimental setup for this series of tests is pictured in figure 2. The input to the primary and reference consisted of the same white Gaussian noise, low-pass filtered at 600 Hz. Prior to each run, the ANC filter weights were initialized to zero. A spectrum analyzer and X-Y plotter were used to plot the input (primary) and output spectra both before and after cancellation.

During convergence, the output voltage was recorded with an RMS voltmeter and plotted as a function of time. The time constant  $\tau$  was measured by fitting the curve  $Ae^{-t/\tau} + A_0$  to this output. Since  $A_0$ , the minimum mean square error, was small, this was approximately the time required for the ANC output to drop to  $(1/e)$  of its initial value (see fig 3).

A summary of the parameter values used in the various tests in this series appear in figure 4. For each test, a plot was made of  $\tau$  versus the pertinent dependent parameter and compared to equation (1).

## TEST RESULTS

Test 1.1 measured  $\tau$  as a function of  $\mu$  for fixed  $N = 64$ ,  $\Delta_p = 32$ , and  $V_{RMS} = 1.56$ . The theoretical dependence is given in appendix A, equation (A-10). Figure 5, a plot of the results, shows excellent agreement between experiment and theory.

In test 1.2,  $\tau$  was measured as a function of  $N$  with fixed  $\mu$  and  $V_{RMS}$ .  $\Delta_p$  was set equal to  $N/2$ . The reasons for this are discussed in the following paragraph. As seen from equation (A-10),  $\tau$  should exhibit no dependence on  $N$ . This was borne out by the results, which are plotted in figure 6.

Test 1.3 examined the performance of the ANC as a function of the delay  $\Delta_p$ . The other parameters were fixed:  $\mu = 2^{-12}$ ,  $N = 64$ ,  $V_{RMS} = 1.58$ . With an infinite filter length, the ANC would show no dependence on  $\Delta_p$ ; however, a finite-length filter cannot model arbitrarily long delays (ref 3). Figure 7 contains a plot of the magnitude of the ANC transfer function at 500 Hz versus the delay. Because of end effects, one would expect optimal cancellation for  $\Delta_p = N/2$ , one half the filter length. For  $\Delta_p > N$ , the delay cannot be modelled by the filter and no cancellation occurs. On the other hand,  $\Delta_p$  should not affect the time constant of the ANC provided it is measurable. This is possible as long as there is some observed cancellation. These remarks are in agreement with figure 8, which plots  $\tau$  versus  $\Delta$ .

In test 1.4,  $\tau$  was measured as a function of the reference voltage  $V_{RMS}$ . The parameters  $\mu$ ,  $N$ , and  $\Delta_p$  were fixed at  $2^{-12}$ , 64, and 32 respectively. The reference voltage was incremented at steps of 3 dB. For values below -12 dB, the cancellation was incomplete. This was caused by the inability of the filter weights to provide enough gain to raise the reference input to the level of the primary. For these values, it was not possible to accurately measure  $\tau$ . The results are plotted in figure 9 and once again show excellent agreement with theory.



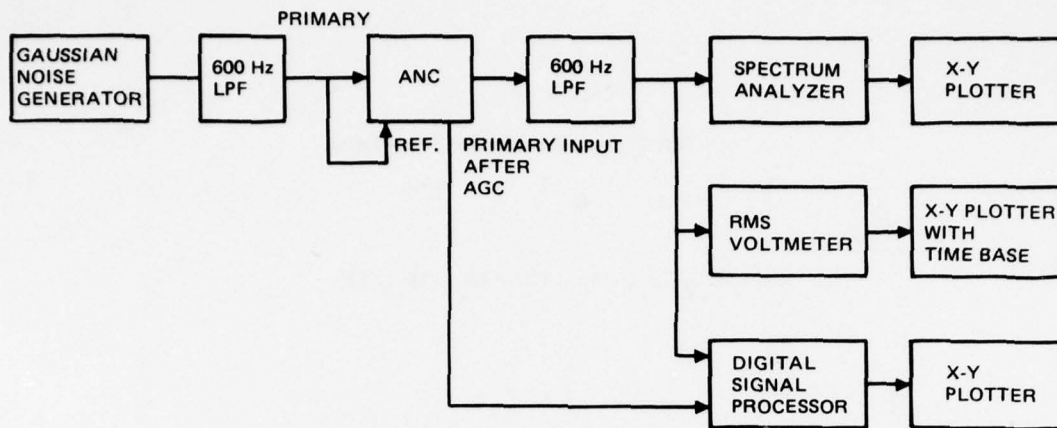


Figure 2. Experimental setup for Test Series 1.

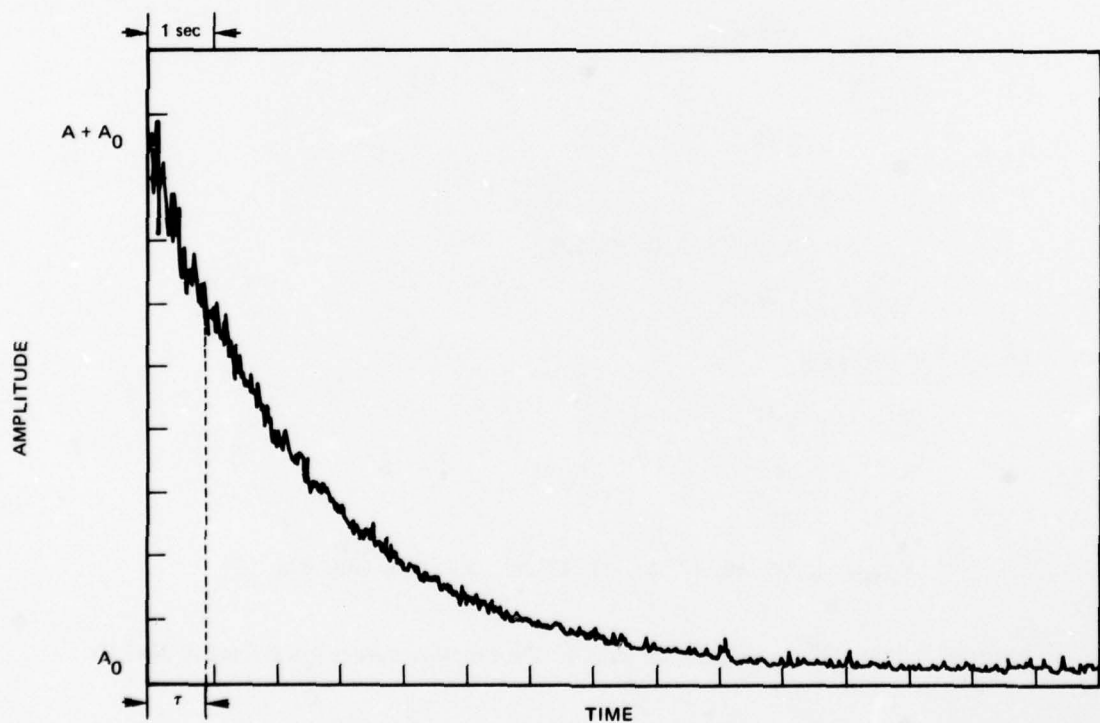


Figure 3. Example of the determination of  $\tau$  from the output voltage.

# Test 1. Broadband Noise Cancellation

## 1.1 $\tau$ versus $\mu$

$$\mu = 2^{-8}, 2^{-9}, 2^{-10}, 2^{-11}, 2^{-12}, 2^{-13}, 2^{-14}, 2^{-15}$$

$$N = 64$$

$$\Delta_p = 32$$

$$V_{\text{RMS}} = 1.56 \text{ volts}$$

## 1.2 $\tau$ versus $N$

$$\mu = 2^{-12}$$

$$N = 16, 64, 256, 1024, 1964$$

$$\Delta_p = N/2$$

$$V_{\text{RMS}} = 1.58 \text{ volts}$$

## 1.3 $\tau$ versus $\Delta$

$$\mu = 2^{-12}$$

$$N = 64$$

$$\Delta_p = 0, 16, 32, 63, 64, 65, 128$$

$$V_{\text{RMS}} = 1.58 \text{ volts}$$

## 1.4 $\tau$ versus $V_{\text{RMS}}$

$$\mu = 2^{-12}$$

$$N = 64$$

$$\Delta_p = 32$$

$$V_{\text{RMS}} = .95, .66, .47, .33, .23, .17, .12, .087, .064, .049, .038, .031$$

Figure 4. Outline of parameters for test series 1. The sample frequency  $f_s$  was fixed at 2048 Hz.

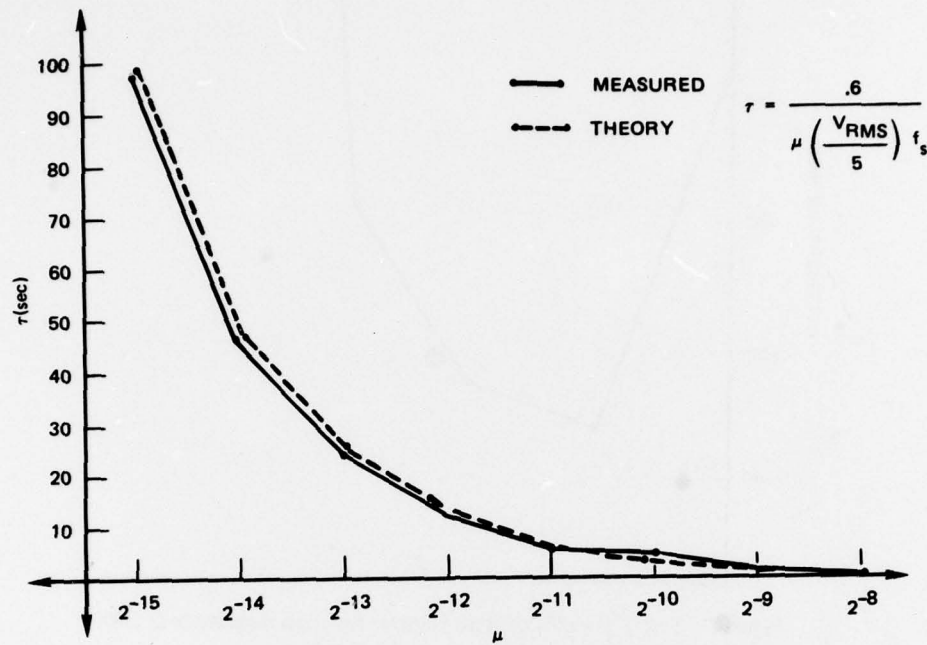


Figure 5. Test 1.1 – plot of  $\tau$  versus  $\mu$ .

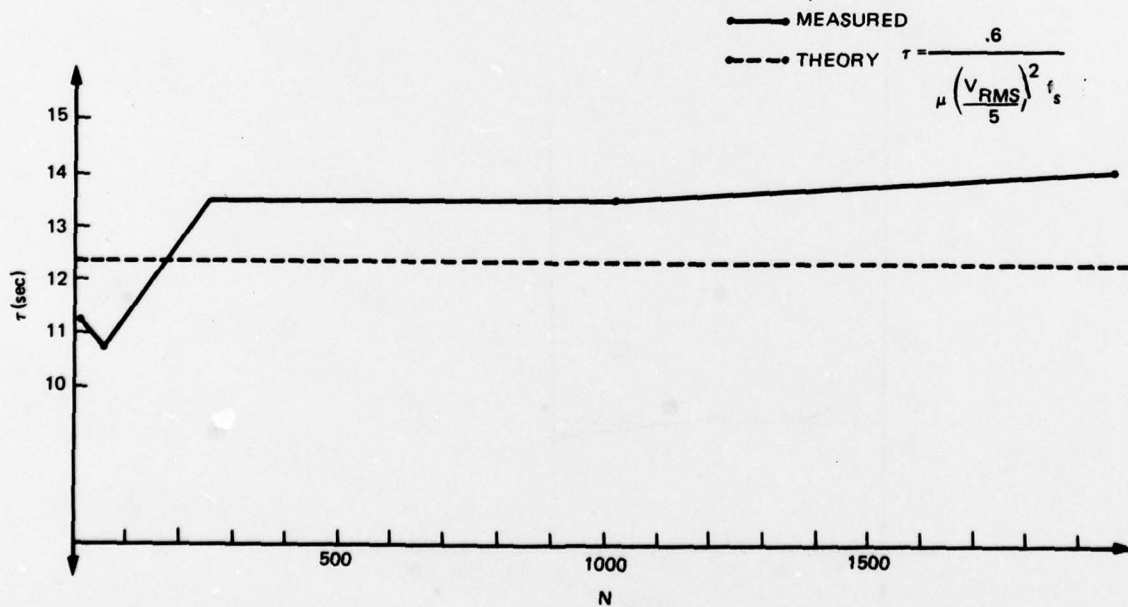


Figure 6. Test 1.2 – plot of  $\tau$  versus  $N$ .

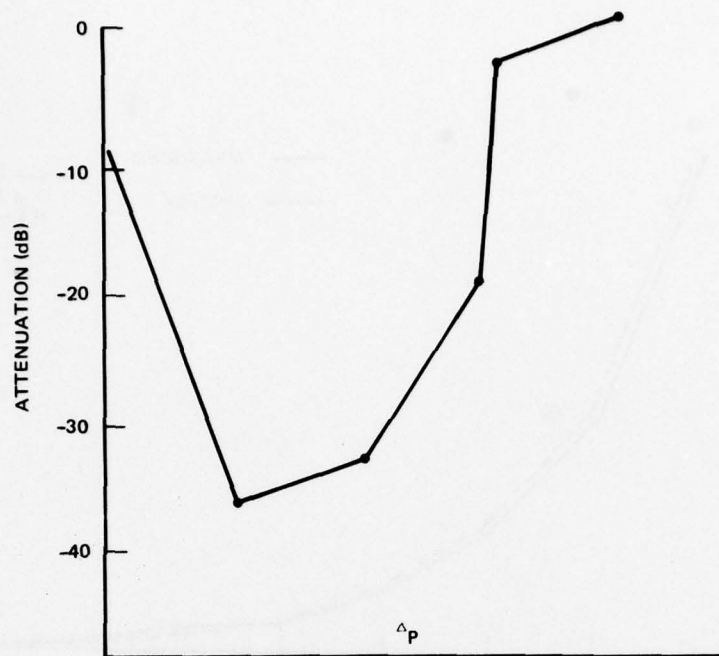


Figure 7. Test 1.3 — plot of ANC transfer function magnitude at 500 Hz versus delay (in units of filter taps) for  $N = 64$ .

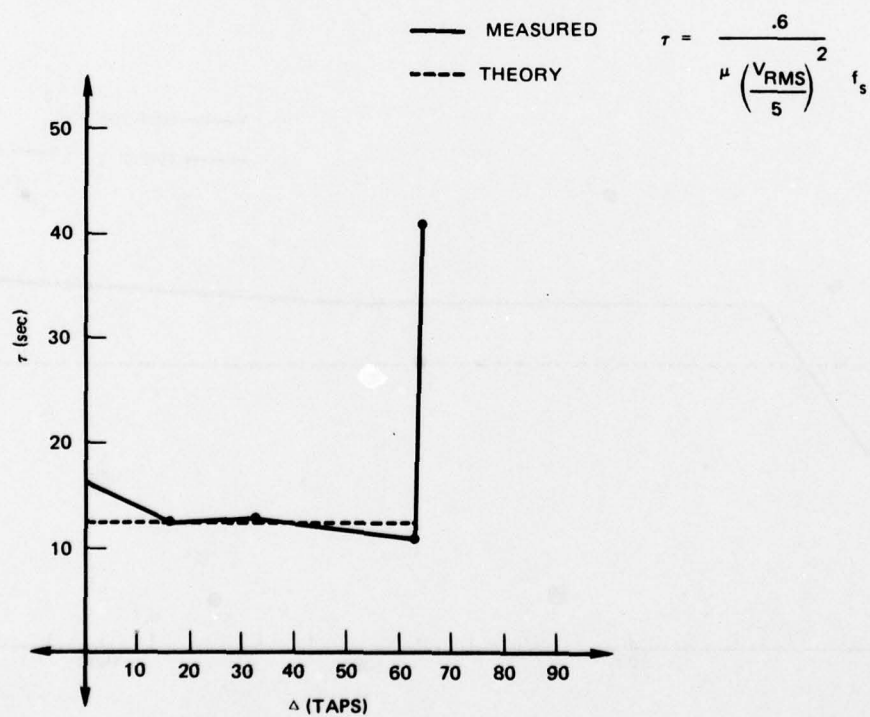


Figure 8. Test 1.3 — plot of  $\tau$  versus  $\Delta_P$ .



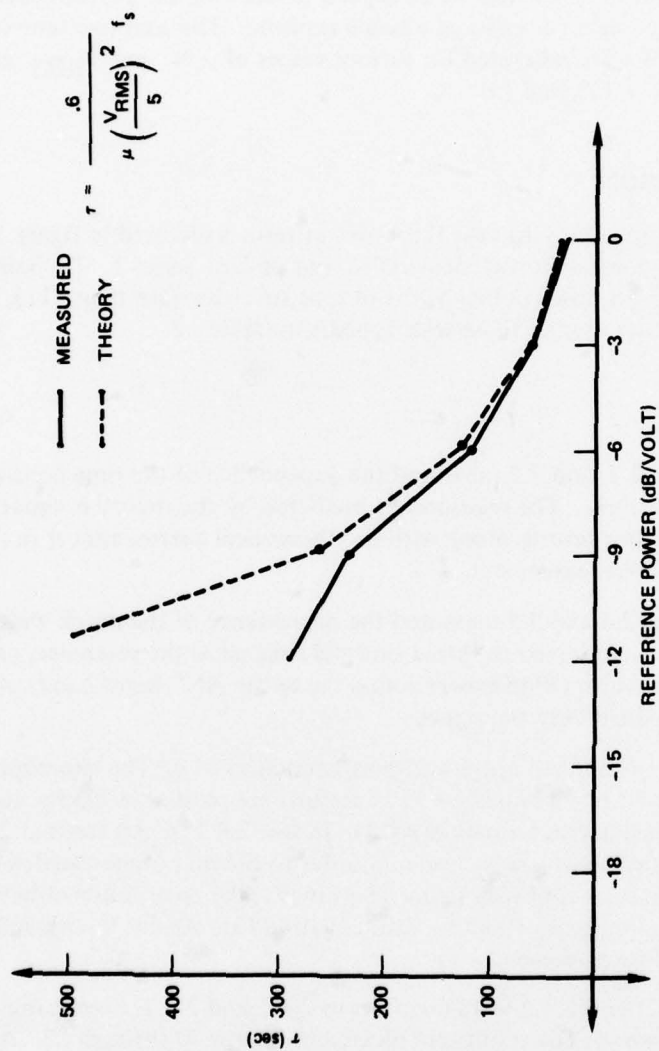


Figure 9. Test 1.4 - plot of  $\tau$  versus the reference voltage,  $V_{RMS}$ .

### III. TEST SERIES 2 – NARROWBAND CANCELLATION

#### TEST OBJECTIVE

The second series of tests was designed to examine the performance of the ANC when the reference signal consists of a single sinusoid. The adaptive time constant  $\tau$  and the notch width  $W$  were measured for various values of  $\mu$ ,  $N$ , and  $V_{RMS}$  in an attempt to verify equations (1), (2), and (3).

#### TEST DESCRIPTION

The experimental setup for this series of tests is pictured in figure 10. The measurement of the time constant  $\tau$  was identical to that of Test Series 1. The notch widths were measured at the 3 dB down points of the output spectrum (see figure 11). A summary of the parameter values used in these tests appears in figure 12.

#### TEST RESULTS

Tests 2.1, 2.2, and 2.3 measured the dependence of the time constant  $\tau$  on  $\mu$ ,  $N$ , and  $V_{RMS}$  respectively. The relationship predicted by the theory is equation (A-2) of appendix A. The test results, along with the theoretical curves, appear in figures 13 through 15 and show excellent agreement.

Test series 2.4 and 2.5 measured the dependence of the notch width,  $W$ , on  $\mu$  and  $N$ . In 2.4 the primary contained the same sinusoidal signal as the reference, plus additive noise at a signal-to-noise ratio (RMS power across the entire ANC input band) of 0 dB. In 2.5, the primary contained only the signal.

Test 2.4.1 examined notch width as a function of  $\mu$ . The experiment was repeated for two values of  $N$ :  $N = 32$  and  $N = 512$ . Results are plotted in figures 16 and 17 along with the theoretical curves (equation A-13). In test 2.4.2,  $\mu$  was fixed at  $2^{-8}$  and  $N$  was varied. The large value of  $\mu$  was chosen in order to obtain notches sufficiently broad to measure. These results appear in figure 18. Finally, the data points obtained are plotted versus  $\tau_{theoretical}$  in figure 19 along with equation (3). Again, theory and experiment are consistently in close agreement.

Tests 2.5.1 and 2.5.2 were identical to 2.4.1 and 2.4.2, except that the signal was absent in the primary. The results are plotted in figures 20 through 23. As may be observed, the absence of the signal in the primary had no effect on the notch width.

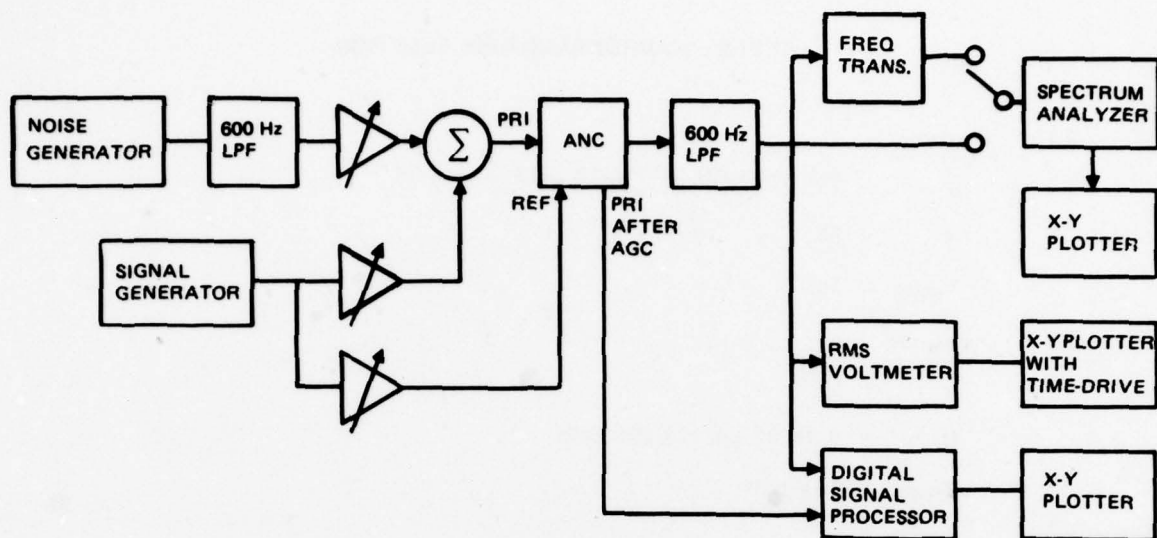


Figure 10. Experimental setup for test 2.1 through test 2.5 the signal was a sine wave at 224.75 Hz.

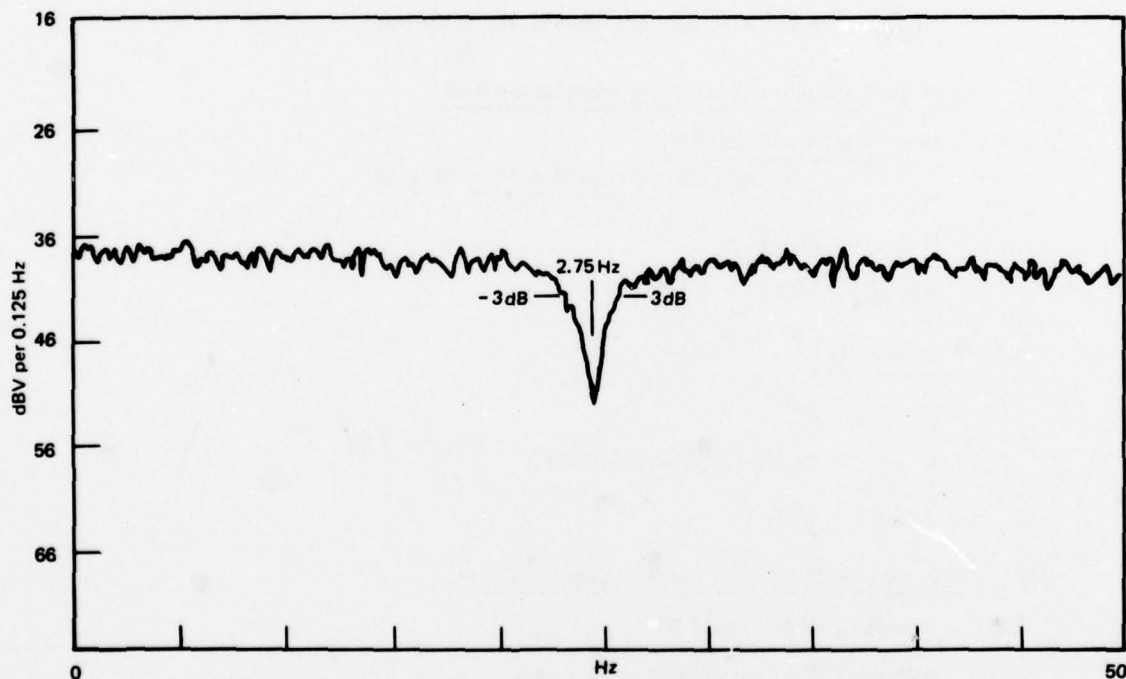


Figure 11. Example of the measurement of notch width (3 dB down point) for test series 2.

## TEST 2 – NARROWBAND CANCELLATION

### 2.1 $\tau$ versus $\mu$

$$\mu = 2^{-8}, 2^{-9}, 2^{-10}, 2^{-11}, 2^{-12}, 2^{-13}, 2^{-14}, 2^{-15}$$

$$N = 64$$

$$V_{\text{RMS}} = 1.8$$

### 2.2 $\tau$ versus N

$$\mu = 2^{-15}$$

$$N = 8, 16, 32, 64, 128, 256, 512$$

$$V_{\text{RMS}} = 1.15 \text{ volts}$$

### 2.3 $\tau$ versus $V_{\text{RMS}}$

$$\mu = 2^{-15}$$

$$N = 64$$

$$V_{\text{RMS}} = 1.5, 1., .74, .52, .37, .26, .18, .13, .1, .07 \text{ volts}$$

### 2.4 W versus N and $\mu$ ; primary signal-to-noise ratio = 0 dB

#### 2.4.1 W versus $\mu$ (two values of N)

$$\mu = 2^{-8}, 2^{-9}, 2^{-10}, 2^{-11}, 2^{-12}, 2^{-13}, 2^{-14}, 2^{-15}$$

$$N = 32, 512$$

$$V_{\text{RMS}} = 1.05$$

#### 2.4.2 W versus N

$$\mu = 2^{-8}$$

$$N = 32, 64, 128, 256, 512, 1024$$

$$V_{\text{RMS}} = 1.2 \text{ volts}$$

### 2.5 W versus N and $\mu$ ; primary signal-to-noise ratio = $-\infty$

#### 2.5.1 W versus $\mu$ (two values of N)

Identical to 2.4.1 except  $V_{\text{RMS}} = 1.1 \text{ volts}$

#### 2.5.2 W versus N

Identical to 2.4.2 except  $V_{\text{RMS}} = 1.8 \text{ volts}$

Figure 12. Parameters for test series 2. The sample frequency was set at  $f_s = 2048$ , the delay at  $\Delta_p = N/2$ , one-half the filter length and the signal frequency 225 Hz.



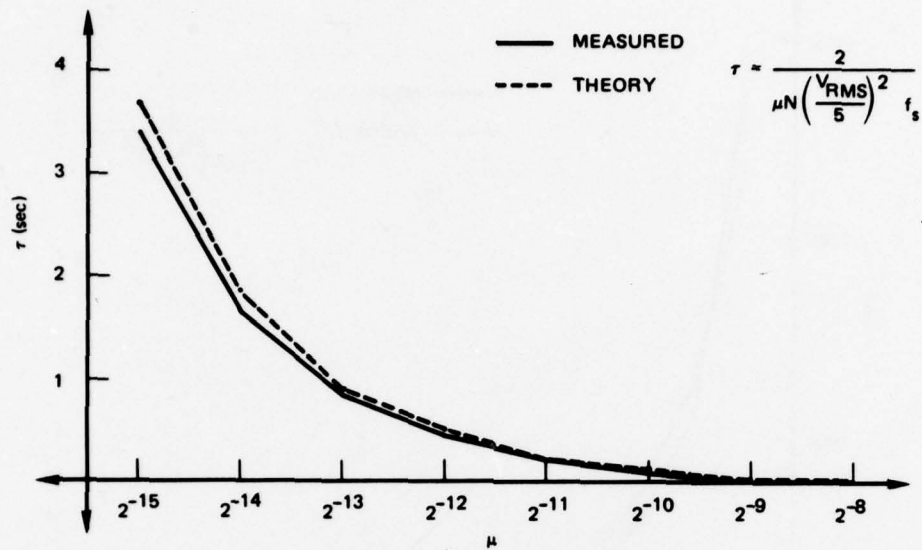


Figure 13. Test 2.1 – plot of  $\tau$  versus  $\mu$ .

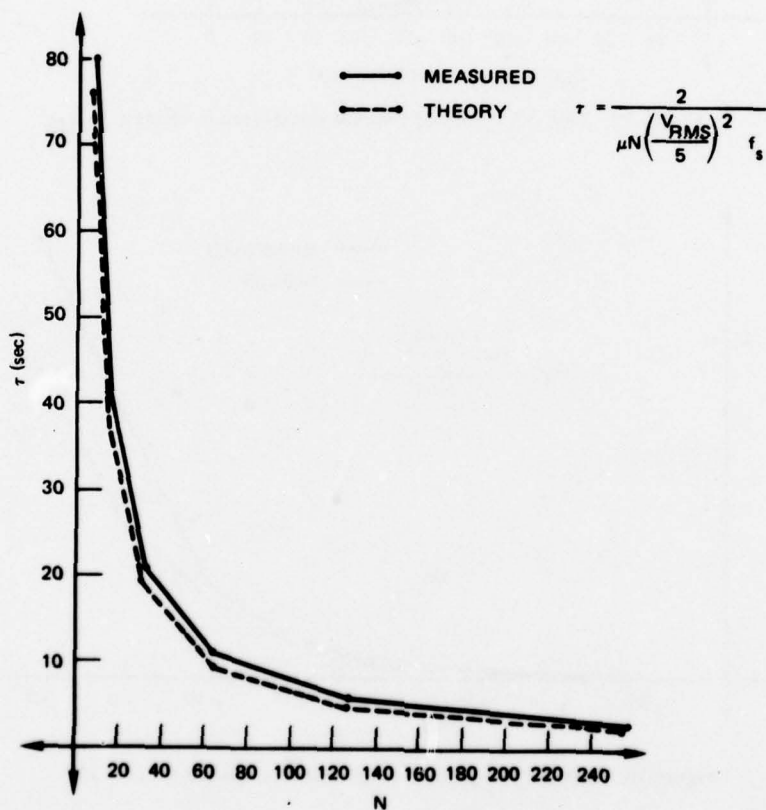


Figure 14. Test 2.2 – plot of  $\tau$  versus  $N$ .

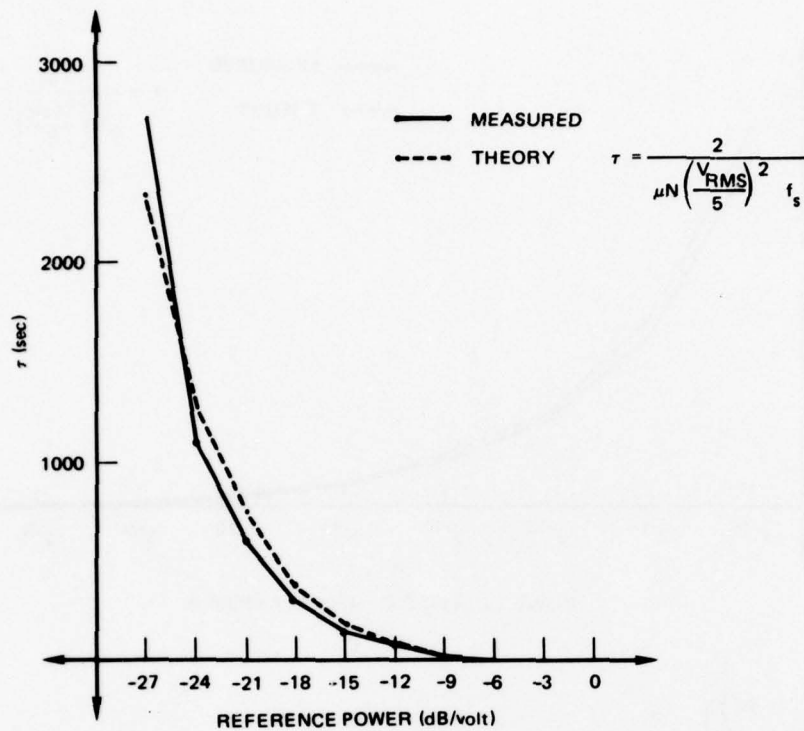


Figure 15. Test 2.3 – plot of  $\tau$  versus the reference voltage,  $V_{RMS}$ .

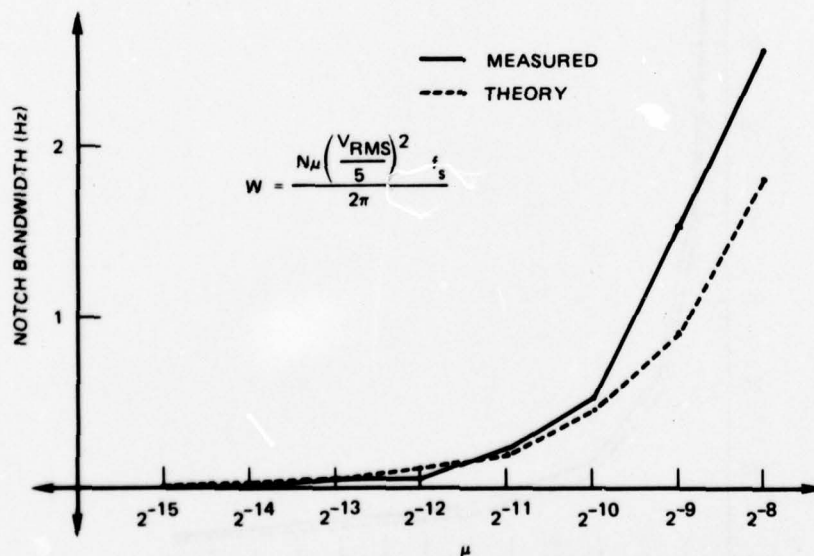


Figure 16. Test 2.4.1 – plot of notch width versus  $\mu$  with  $N = 32$ .

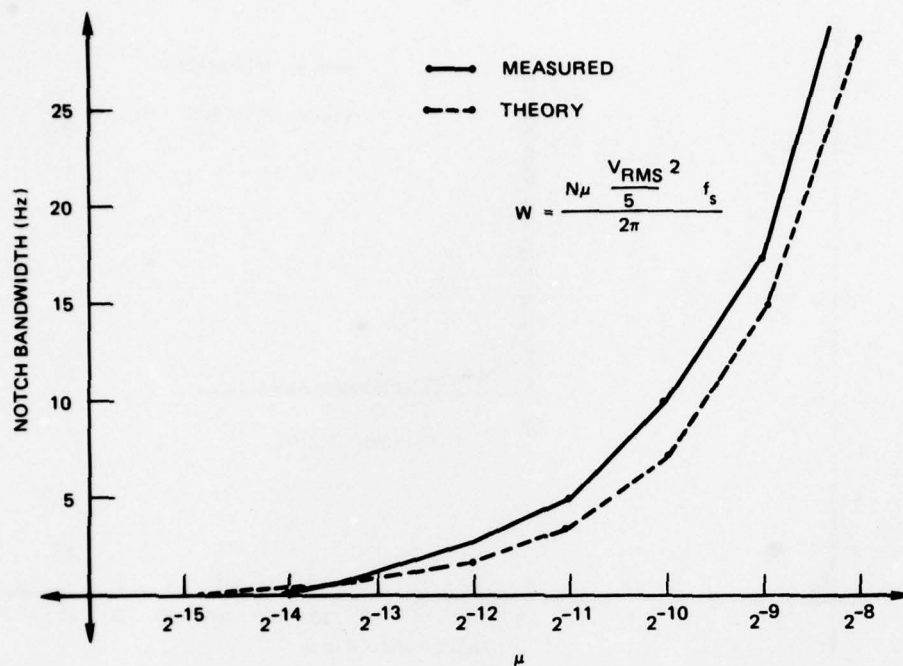


Figure 17. Test 2.4.1 – plot of notch width versus  $\mu$  with  $N = 512$ .

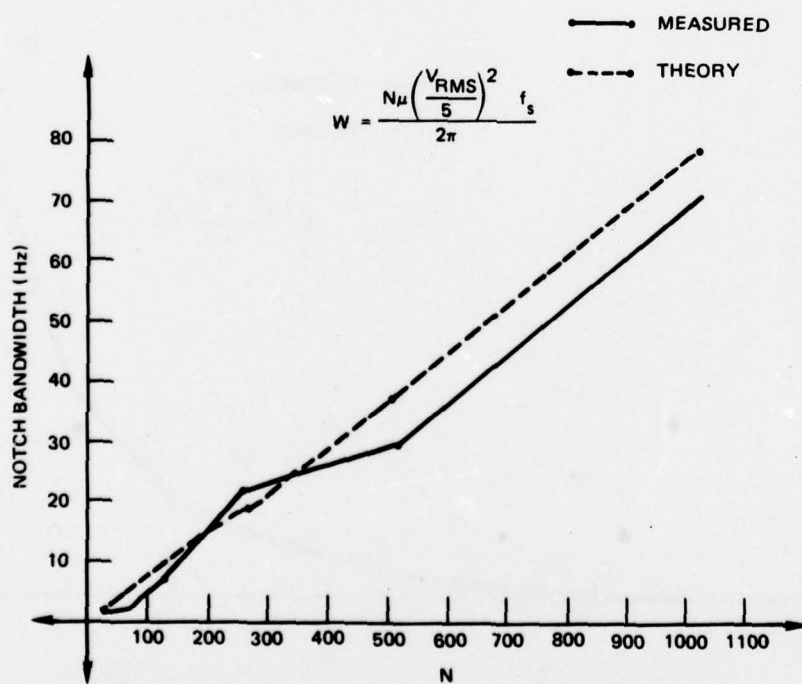


Figure 18. Test 2.4.2 – notch width versus  $N$  with  $\mu = 2^{-8}$ .

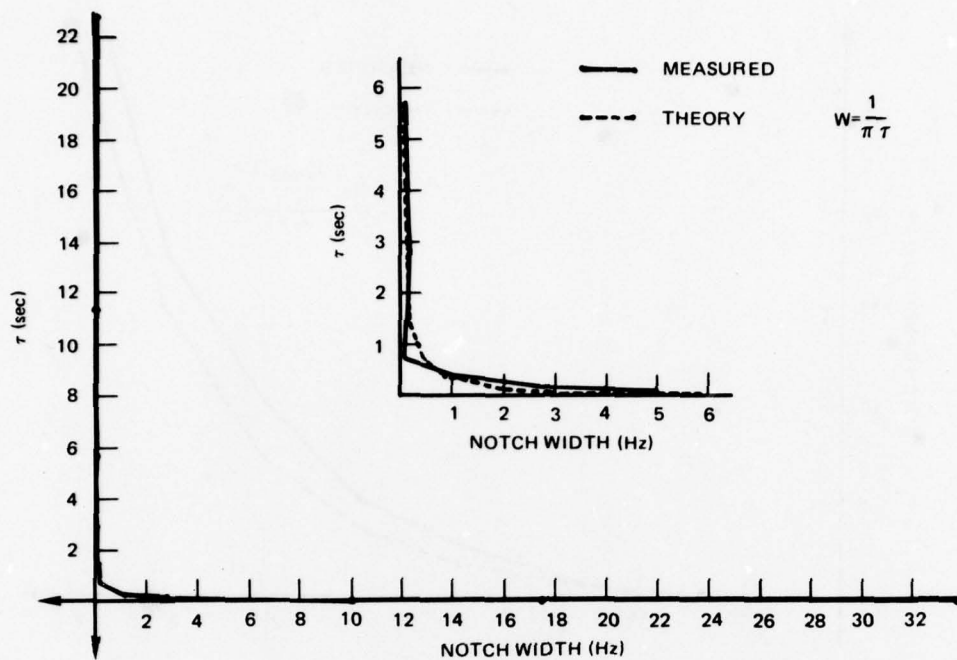


Figure 19. Test 2.4 – plot of notch width versus  $\tau$ . The data points were taken from 2.4.1 and 2.4.2. For clarity a portion of the plot has been redrawn at a magnified scale.

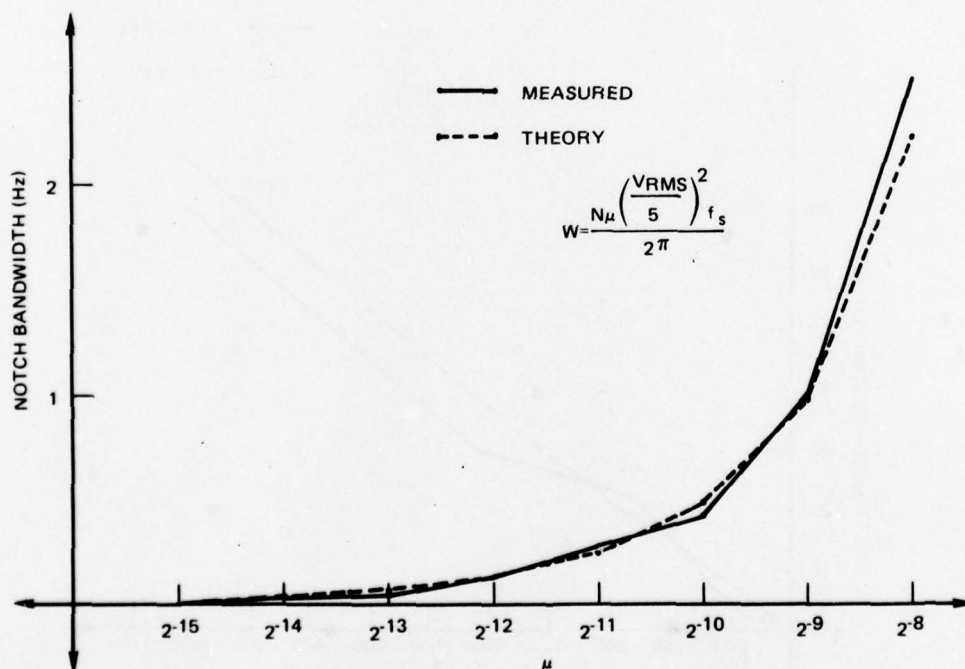


Figure 20. Test 2.5.1 – plot of notch width versus  $\mu$  for  $N = 32$ .



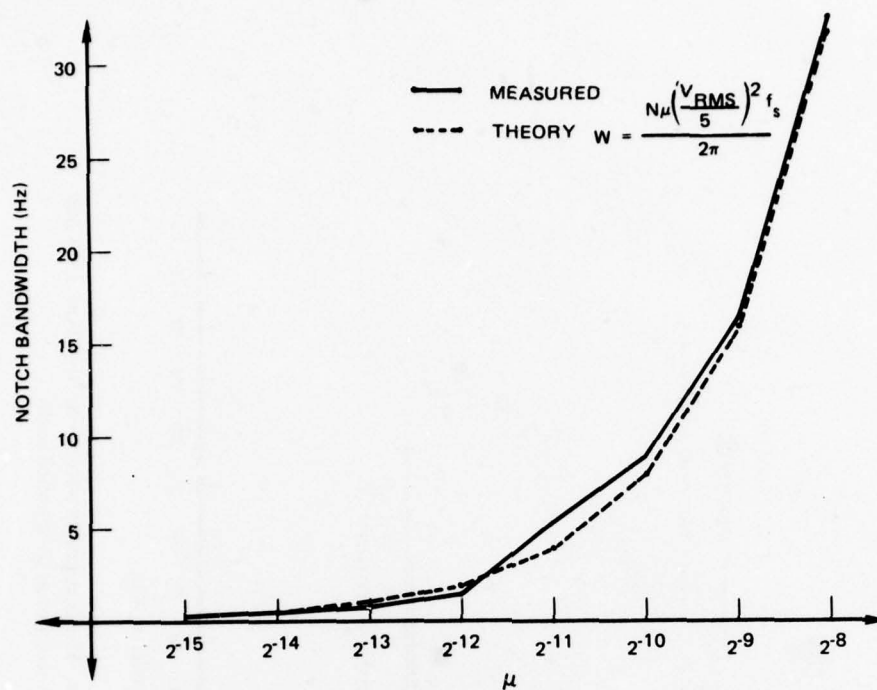


Figure 21. Test 2.5.1 – plot of notch width versus  $\mu$  for  $N = 512$ .

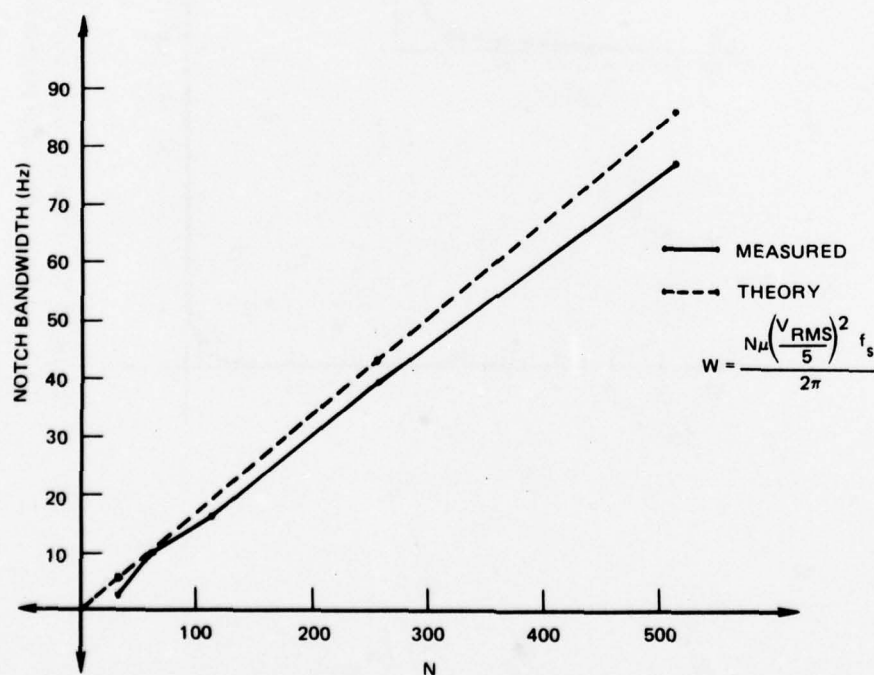


Figure 22. Test 2.5.2 – plot of notch width versus  $N$  for  $\mu = 2^{-8}$ .

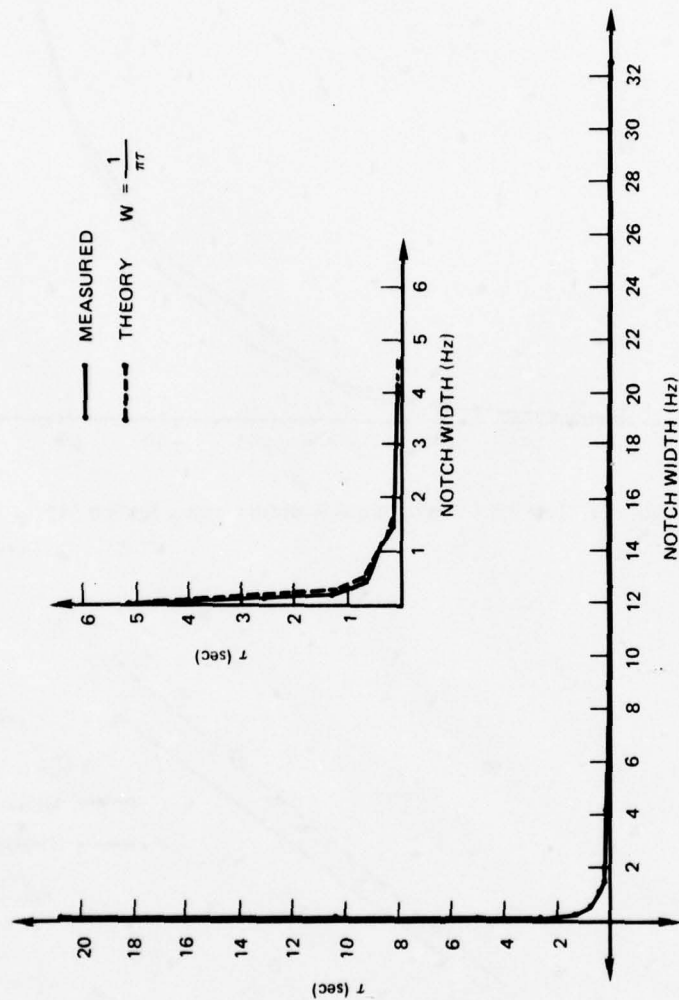


Figure 23. Test 2.5 plot of notch width versus  $\tau$ . The data points were taken from both 2.5.1 and 2.5.2. For clarity a portion of the plot has been redrawn at a magnified scale.

#### IV. TEST SERIES 3 - MULTIPLE LINES

##### TEST OBJECTIVE

This series of tests examined the behavior of the noise canceller for signals containing more than one sinusoid. Time constants, notch widths, and notch depths were measured as a function of the frequency separation  $\Delta f$ , of the signal components.

##### TEST DESCRIPTION

The experimental setups for Test Series 3 are pictured in figures 24 through 27. Figure 28 is a diagram of the ANC with multiple references, which was used in experiment 3.4 in place of the configuration depicted in figure 1.

Slightly different techniques were used to measure the time constants in this series of tests. The noise in the primary (which was not cancelled) overshadowed the output power in test 3.1. In order to make  $\tau$  visible, the level of the frequency cell containing the signal (120 Hz) was monitored. The level was in decibels and  $\tau$  was computed from the formula (see appendix B)  $\tau \sim \frac{t_1 - t_2}{y_2 - y_1} \frac{20}{\ln 10}$ . In 3.3 and 3.4, monitoring was not necessary; however, the noise did tend to obscure the final level. As a result, three points were needed to fit the curve  $Ae^{-t/\tau} + A_0$  and thus determine  $\tau$ .

Notch widths,  $W$ , were measured as in test series 2. The notch depths,  $D$ , of the transfer functions were determined by comparing the input and output spectra of the primary. (To remove the effects of the external 600 Hz filter, the input spectrum was measured at the output by setting the reference voltage to zero.) More precisely, the notch depths are given by

$$D = \frac{\text{primary output power in dBV at signal frequency}}{\text{primary input power in dB at signal frequency}}$$

The parameter values used in Test Series 3 appear in figure 29.

##### TEST RESULTS

Test 3.1 measured the time constant  $\tau$ , notch width  $W$ , and notch depth  $D$  as a function of frequency separation  $\Delta f$  of two sinusoids in the reference. One frequency was held constant at 120 Hz and the other varied from 170 Hz to 120.5 Hz. The 120 Hz tone was also present in the primary.

In all cases two notches were visible, at the two reference frequencies. For separation of less than 10 Hz, the notch widths were not measurable. These results are tabulated in table 1. The absolute notch depths,  $d_i$ , of the primary output spectrum are included as well as the notch depths,  $D_i$ , of the transfer function. The depths  $d_1$  and  $d_2$  appear to be

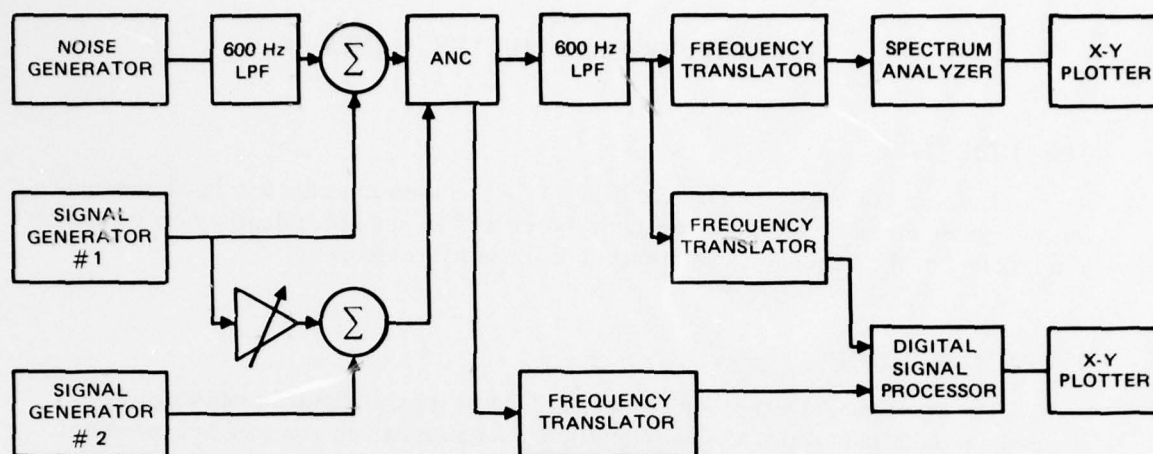


Figure 24. Experimental setup for test 3.1.

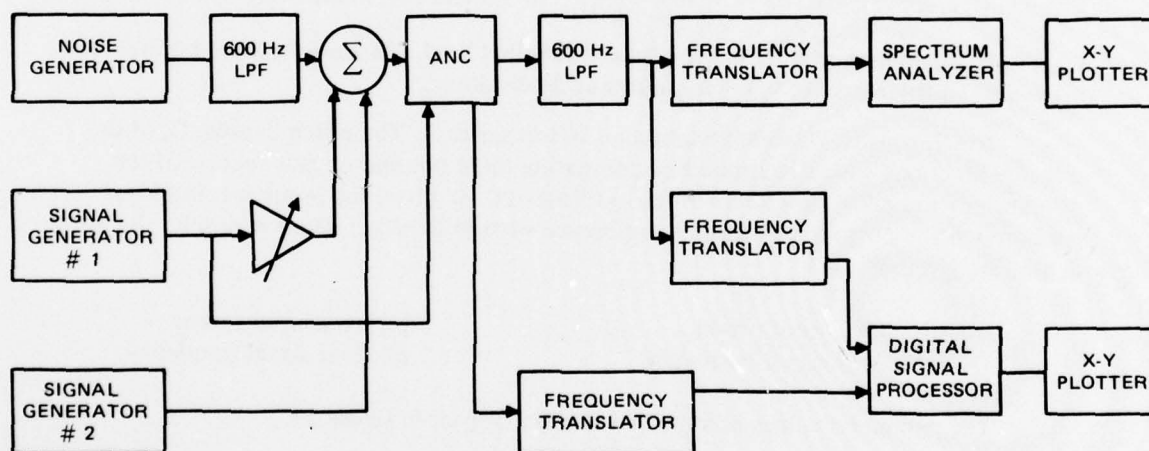


Figure 25. Experimental setup for test 3.2.



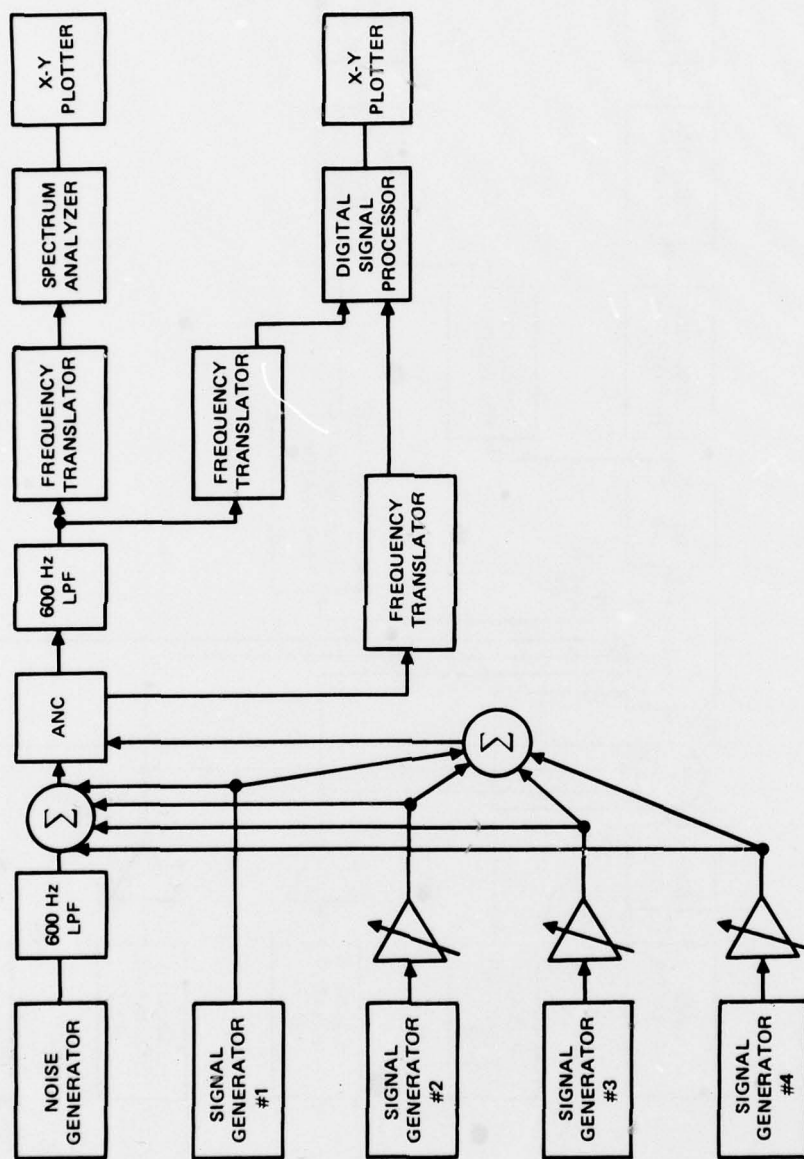


Figure 26. Experimental setup for test 3.3.

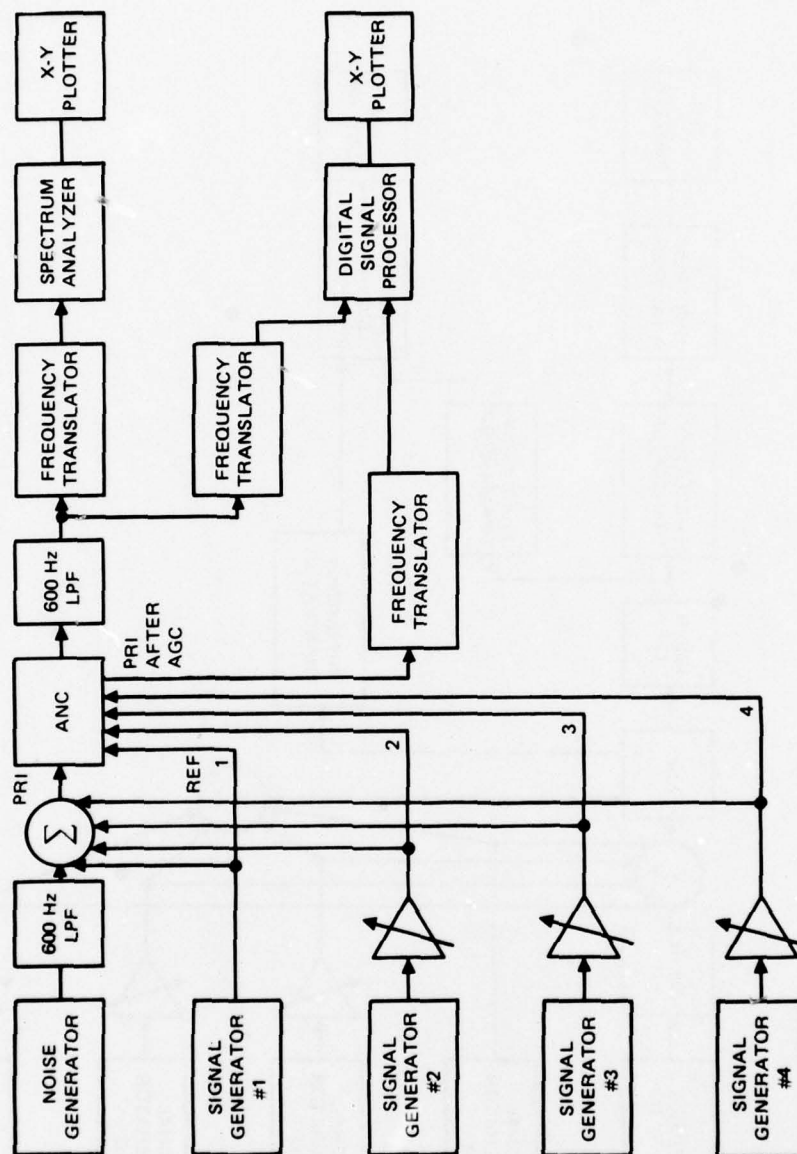


Figure 27. Experimental setup for test 3.4.

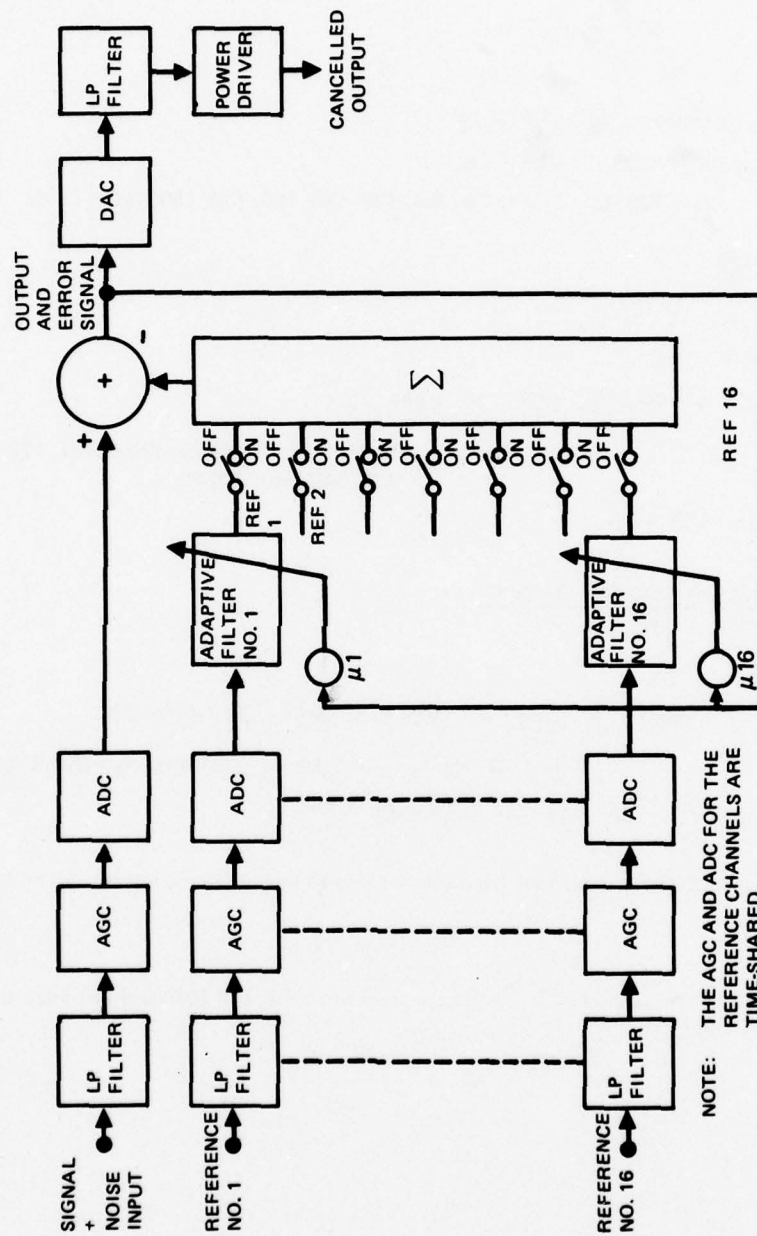


Figure 28. Block diagram of multiple reference ANC.

### TEST 3

#### 3.1 $\tau, W, D$ versus $\Delta f$

$$\begin{aligned}\mu &= 2^{-8} \\ N &= 64\end{aligned}$$

$$\text{Primary: } V_{\text{noise}} = .72 \quad V_1^{\text{sig}} = .75$$

$$\text{Reference: } V_1^{\text{sig}} = .78 \quad V_1^{\text{sig}} = .78$$

$$f_1 = 120 \text{ Hz} \quad f_2 = 120.5, 121, 122, 123, 125, 130, 140, 150, 170 \text{ Hz}$$

#### 3.2 $W$ versus $\Delta f$

$$\begin{aligned}\mu &= 2^{-12} \\ N &= 64\end{aligned}$$

$$\text{Primary: } V_{\text{noise}} = .79 \quad V_1^{\text{sig}} = .39 \quad V_2^{\text{sig}} = .79$$

$$f_1 = 120 \text{ Hz} \quad f_2 = 119.5, 119.75, 120.25, 120.5, 121, 122, 123, 125, 130, 140, 150, 170 \text{ Hz}$$

$$\text{Reference: } V_1^{\text{sig}} = .39$$

#### 3.3 $\tau, W, D$ for four signals in reference

$$\begin{aligned}\mu &= 2^{-12} \\ N &= 64\end{aligned}$$

$$\text{Primary: } V_{\text{noise}} = .49 \quad V_1^{\text{sig}} = .37 \quad V_2^{\text{sig}} = .36 \quad V_3^{\text{sig}} = .36 \quad V_4^{\text{sig}} = .37$$

$$f_1 = 201 \text{ Hz} \quad f_2 = 201.1 \text{ Hz} \quad f_3 = 201.2 \text{ Hz} \quad f_4 = 201.3 \text{ Hz}$$

$$\text{Reference: } V_1^{\text{sig}} = .36 \quad V_2^{\text{sig}} = .75 \quad V_3^{\text{sig}} = .51 \quad V_4^{\text{sig}} = .41$$

#### 3.4 Identical to 3.3 except the four signals were input to four different references and $N = 16$ .

Figure 29. Parameters for test series 3. The sample rate was set at  $f_s = 2048$  and the delay at  $\Delta_p = N/2$ , one half the filter length.



approximately equal at the two reference frequencies. However, the 120 Hz signal in the primary was about 36 dB above the noise level (at a resolution of .125 Hz). Thus, considerably more cancellation occurred for the sinusoid which appeared in both the primary and reference than for the cancellation which occurred in the reference alone; i.e.,  $|D_1|$  was generally 36 dB larger than  $|D_2|$ . Also notice the decrease in cancellation (at both  $f_1$  and  $f_2$ ) with decreasing  $\Delta f$  (especially for  $\Delta f < 10$  Hz); therefore, the above observations may not be explained simply as an infinitely deep notch which was clipped by the electronic equipment.

Table 1. Notch Widths and Notch Depths for Experiment 3.1. The First Signal was at 120 Hz with a Power of -3 dBV. The Noise Level was -38.5 dB/Cell at a Cell Width of .125 Hz. D Indicates Absolute Depth of the Notch; D Shows Cancellation in dB.

$\Delta f$	$f_2$	$W_1$ (Hz)	$W_2$ (Hz)	$d_1$ power/cell dBV	$d_2$ power/cell dBV	$D_1$ dBV	$D_2$ dBV
50	170	2.8	—	-57	—	-54	—
30	150	2.0	2.0	-59	-63	-56	-25
20	140	1.3	1.6	-55	-56	-52	-18
10	130	.8	1	-48	-48	-45	-10
5	125	—	—	-43	-41	-40	-3
3	123	—	—	-42	-42	-39	-4
2	122	—	—	-44	-45	-41	-7
	121	—	—	-38	-38	-35	0
.5	120.5	NOT CONVERGED					

According to the theory in reference 4, two time constants should be present, with values given by

$$\tau_{\pm} = \frac{1}{2\mu \sigma_s^2 f_s \lambda_{\pm}},$$

where

$$\lambda_{\pm} = \frac{N}{2} \pm \frac{|Z|}{2}$$

and

$$Z = \frac{\sin \frac{\pi N}{f_s} \Delta f}{\sin \frac{\pi}{f_s} \Delta f} \quad (4)$$

4. NOSC Working Paper, Time Constants and Learning Curves of LMS Adaptive Filters (U), by M Shensa, Unclassified, 1979

For large frequency separations, the time constants  $\tau_+$  and  $\tau_-$  are approximately equal with values given by substituting  $\lambda = N/2$ . For small  $\Delta f$ , however, they are very different; the fast time constant has  $\lambda = N$  (twice as fast as when  $\Delta f$  is large). Note that this is the same as (A-2) with  $V_{RMS}^2$  replaced by the total signal power. The slow time constant is proportional to  $(\Delta f)^{-2}$  (more precisely  $\lambda_-$  is about  $\pi^2 N^3 (\Delta f)^2 / (12 f_s^2)$ ).

Both time constants were observed in the present test. An example appears in figure 30. The system response time prevented accurate measurement of the fast time constant,  $\tau_+$ ; however, considerable success was achieved for the slower time constant,  $\tau_-$ . The results appear in table 2 and figure 31 (note that  $\hat{\mu} = \mu/2$ ).

Table 2. Time Constants Versus Frequency Separation for Test 3.1, Theoretical and Measured Values

$\Delta f$ Hz	$\tau_+$ sec	$\tau_-$ sec	$\tau_-$ (measured) sec
.5	.08	401	530
1	.08	97	100
2	.08	24	21
3	.088	6.1	3
5	.083	2.7	—
10	.09	1.0	—
20	.11	.29	.2
30	.13	.20	.2
50	.13	.20	.17

The configuration in test 3.2 was essentially the same as in test series 2, except for the addition of a second sinusoid in the primary. Notch width was measured as a function of  $\Delta f$ , the signal separation in the primary. In theory, the second signal should have no effect on the notch width. This was confirmed by the results (fig 32), although it should be noted that the measurement accuracy was limited by the narrowness of the notches.

Test 3.3 examined the behavior of the noise canceller for a reference signal consisting of a sum of four sinusoids spaced  $\Delta f = .1$  Hz apart and with relative signal powers of 1, 4, 2, and 1.33. Extrapolating the theory from the case of two closely spaced sinusoids (ref 4), one would expect the fastest time constant to be given by  $\tau = (\mu \sigma^2 N f_s)^{-1}$  where  $\sigma^2$  is the total reference power and  $\hat{\mu} = \frac{\mu}{2}$ , one half the panel setting for  $\mu$ . The actual measured time constant for  $N = 64$  and  $\mu = 2^{-12}$  was 1.8 sec. The total reference voltage was 1.06 volts RMS. When these values ( $\sigma^2 = V^2/25$ ) are substituted in the above formula, one gets 1.6 seconds, in close agreement with the measured value.

On the other hand, the slow time constant should be longer than the fast time constant by a factor of  $12 \left( \frac{f_s}{N \pi \Delta f} \right)^2$ , which is about  $10^5 \times (1.2)$  seconds or 1.4 days. For this

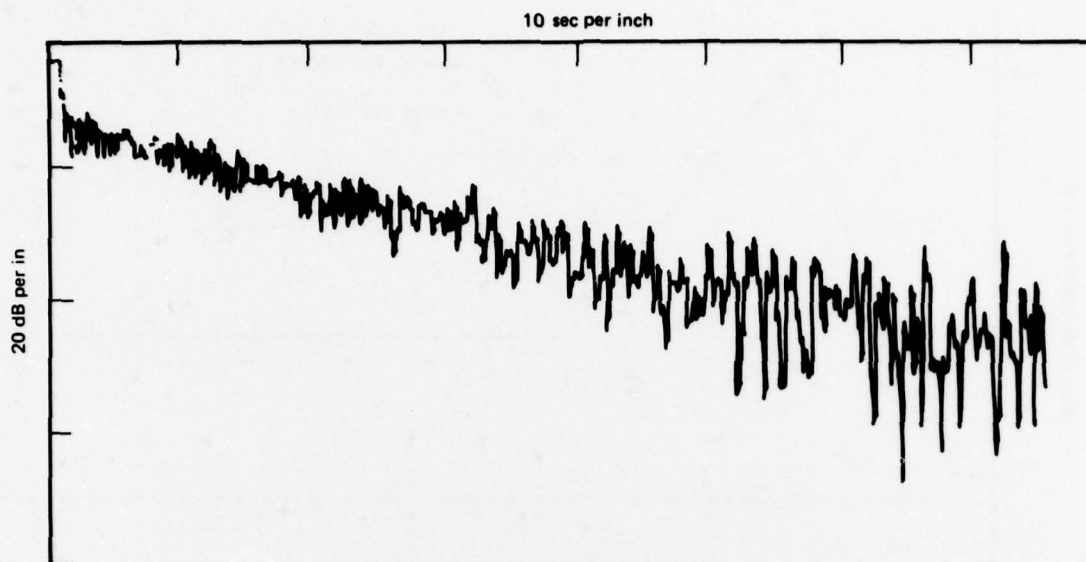


Figure 30. Example of the noise canceller output voltage in test 3.1 for  $\Delta f = 2$  Hz. The appearance of increased variance for low levels is simply due to the logarithmic y-axis.

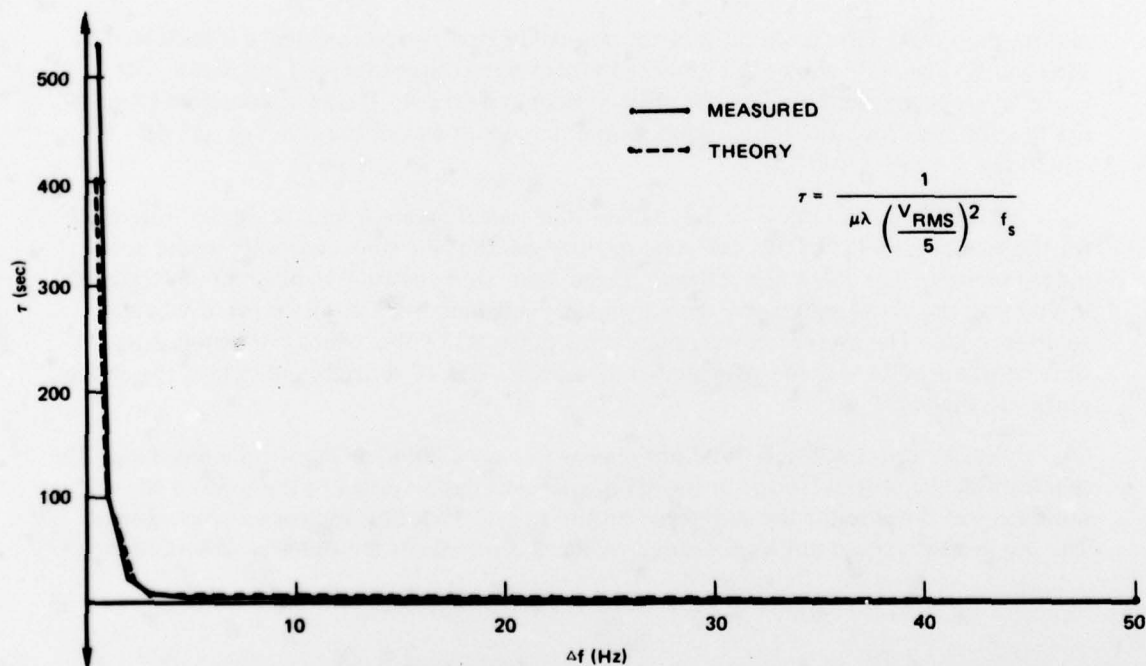


Figure 31. Test 3.1 — plot of decay time,  $\tau$ , as a function of frequency separation  $\Delta f$ .

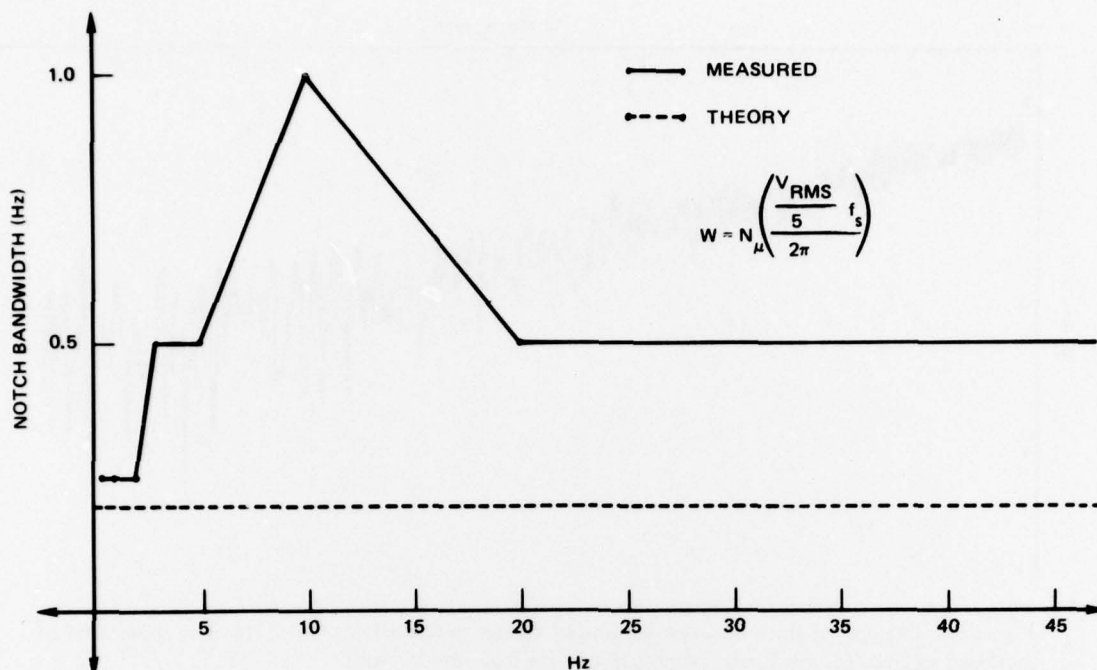


Figure 32. Test 3.2 – plot of notch width as a function of frequency separation in the primary input.

reason, the slower time constant was not observed. However, its existence is indicated by the results. Figure 33 shows the supposedly converged output (several minutes). The cancellation is considerably less (27 dB less) than in Test 3.4. It was not possible to measure the notch width. The transfer function notch depth was of the order of -31 dB  $-(-20 \log .37 \text{ volts}) = -22 \text{ dB}$ .

Test 3.4 was identical to 3.3, except that four separate reference inputs were used for the four sinusoids. In this case, one might guess that the time constants would act independently. The reference voltages ranged from .36 volts to .71 volts. Since  $N$  was 16 in this test, the above values give a range in time constants (equation A-2) of 6 seconds to 48 seconds. The average power/reference input was .5 volts, which corresponds to a time constant of 24 seconds. The actual measured  $\tau$  was 17 seconds and falls in the above range of values.

Unlike test 3.3, test 3.4 did not appear to have a "hidden" slow time constant. The spectrum of the output (found in fig 34) shows cancellation down to the level of the noise (as was the case for the converged output in test 3.1), thus indicating convergence. The notch width could not be measured. Cancellation was of the order of -58  $-(20 \log .32)$ .



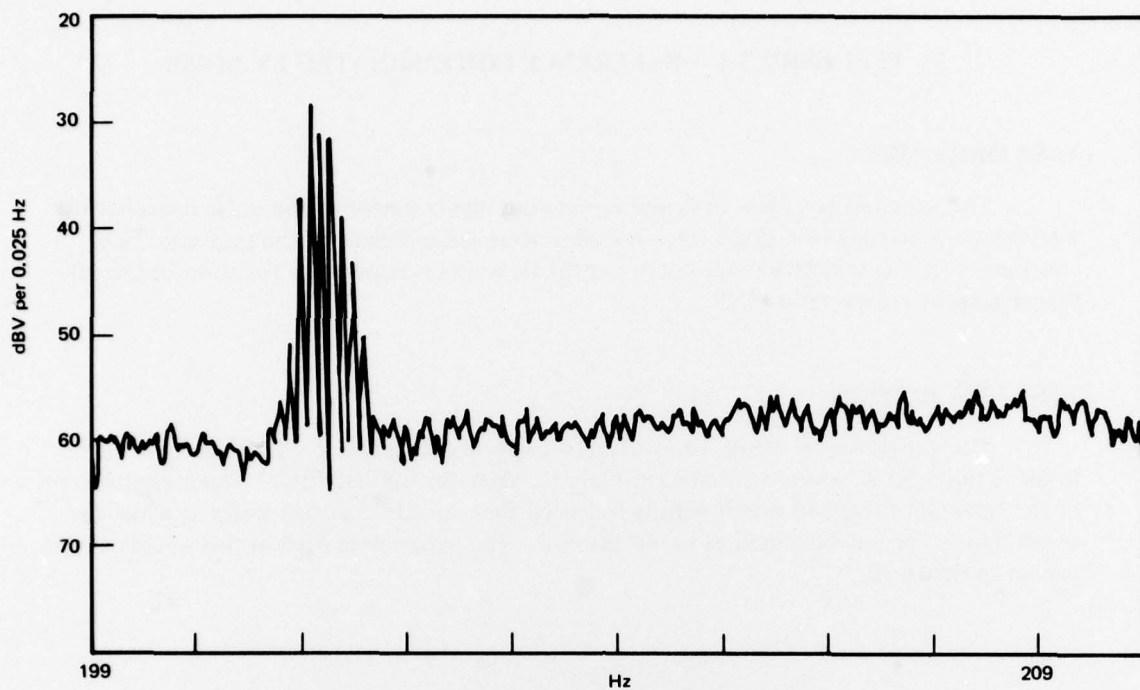


Figure 33. Output spectrum for test 3.4.

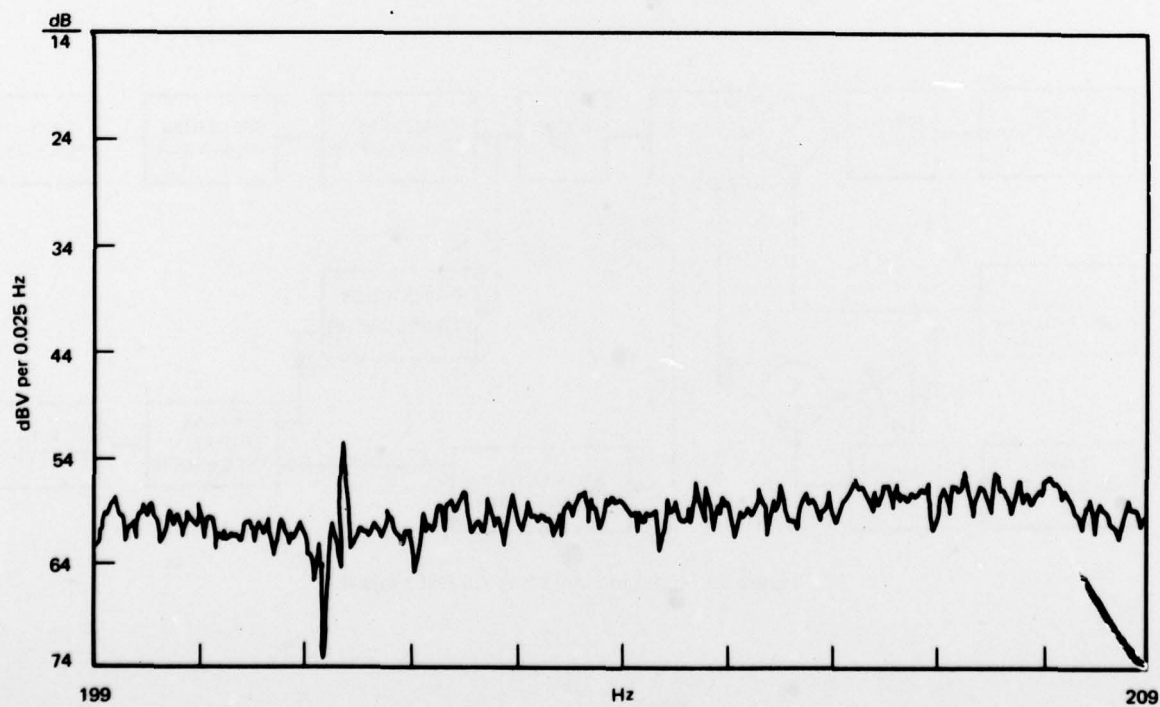


Figure 34. Spectrum of noise canceller output for test 3.4.

## V. TEST SERIES 4 – REFERENCE CONTAMINATED BY NOISE

### TEST OBJECTIVE

This series of tests was designed to examine the behavior of the noise canceller for a reference consisting of a single sinusoid, plus noise independent of the primary. Time constants  $\tau$ , notch widths  $W$ , and notch depths  $D$ , were measured as a function of the reference signal-to-noise ratio, SNR.

### TEST DESCRIPTION

The experimental setup for test series 4 appears in figure 35. The reference signal-to-noise ratio, SNR, was measured as in figure 1, after the 600 Hz filter. The measurement of the time constants and notch widths followed the procedure of test series 2, while the notch depths were determined as in test series 3. The parameters used in this series of tests appear in figure 36.

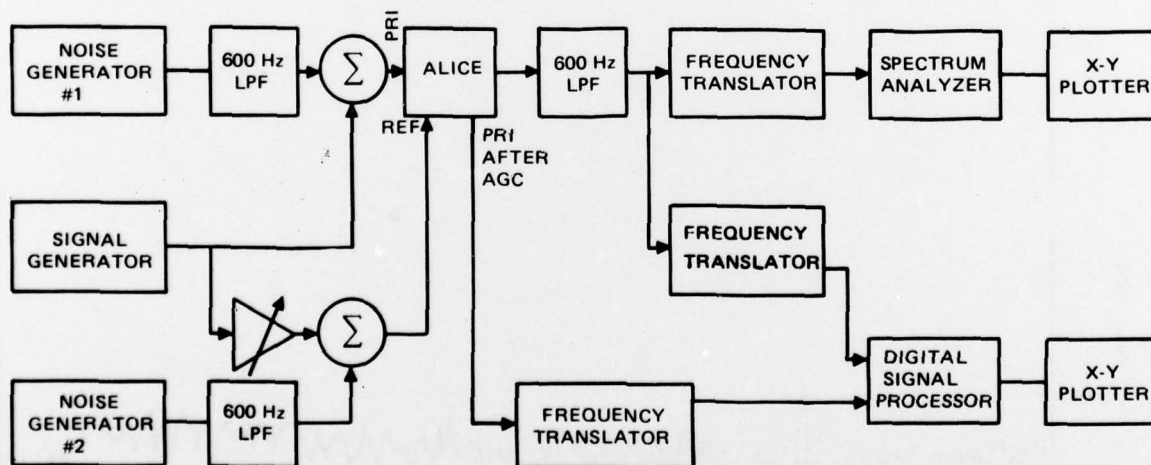


Figure 35. Experimental setup for test series 4.

# TEST 4

## 4.1 $\tau$ versus (SNR) reference

$\mu$	$= 2^{-12}$											
N	$= 64$											
$V_{ref}^{sig}$	$= .99$	$.99$	$.99$	$.99$	$.99$	$.99$	$.7$	$.5$	$.35$	$.25$	$.12$	
$V_{ref}^{noise}$	$= 0$	$.08$	$.12$	$.25$	$.5$	$.99$	$.99$	$.99$	$.99$	$.99$	$.99$	
$V_{prim}^{sig}$	$= .95$											
		$V_{prim}^{noise} = 0$										

## 4.2 W, D versus (SNR)ref

$\mu$	$= 2^{-8}$																	
N	$= 64$																	
$V_{ref}^{sig}$	$= .8$	$.8$	$.8$	$.4$	$.28$	$.2$												
$V_{ref}^{noise}$	$= 0$	$.4$	$.8$	$.8$	$.8$	$.8$												
$V_{prim}^{sig}$	$= .19$																	
		$V_{prim}^{noise} \approx 1.08$																

## 4.3 Identical to 4.2 except for absence of the signal in the primary.

Figure 36. Parameters for test series 4. The sample rate was  $f_s = 2048$  and the delay,  $\Delta_p = N/2$ , was one half the filter length.

## TEST RESULTS

Test 4.1 measured the time constant  $\tau$  as a function of reference signal-to-noise ratio, SNR. The results are plotted in figure 37. They are compared with equation (A-8) in table 3. Although the general tendency (longer time constants for decreasing SNR) is correct, the values differ widely from equation (A-8) for low SNR. This may be due to an inability to measure the effects of the noise on the time constant (since the weights start at zero), which is the converged final value for uncorrelated noise alone in the reference. Or, it may be a failure of the theory to account for the type of behavior described in reference 2.

Test 4.2 measured notch width and depth as a function of signal-to-noise ratio. N was fixed at 64 and  $\mu$  at  $2^{-8}$ . The primary contained both the signal and noise. Wiener filter theory (ref 5) indicates that the formula for notch width, equation (A-13), should remain unchanged; whereas, the notch depth (theoretically/infinite for no noise in the reference) should be given by

$$D = -20 \log \left( 1 + \frac{\sigma_s^2}{\sigma_n^2} \right) \quad (5)$$

5. (NOSC) NUC Working Paper, Adaptive Noise Cancelling and Line Enhancing in Passive Sonar Signal Processing: Theory, Experiment, and Hardware Requirements (U), by P Reeves and D Chabries, Confidential, 1976

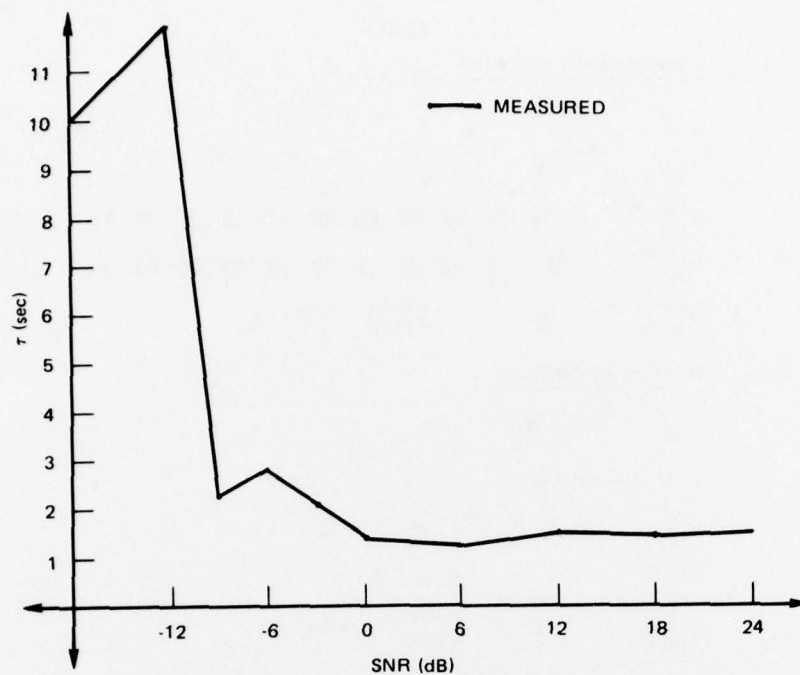


Figure 37. Test 4.1 – plot of  $\tau$  versus SNR, the reference signal-to-noise ratio.

Table 3.  $\tau$  vs SNR for Test 4.1 Compared to Values Computed by Equation (A-8)

Reference SNR in dB	$\tau$ (equation A-8) seconds	$\tau$ (measured) seconds
$\infty$	1.6	1.5
24	1.6	1.5
18	1.6	1.4
12	1.6	1.5
6	1.6	1.3
0	1.6	1.4
-3	2.7	2.1
-6	5.8	2.8
-9	11	2.3
-12	19	12
-18	48	10

The data obtained, plotted in figures 38 and 39, are consistent with these remarks.

Test 4.3 was identical to test 4.4 except that the signal was absent in the primary. The results are plotted in figures 40 and 41. Although the notch width is the same as in Test 3.2, the magnitude of the notch depth is considerably smaller (although still linear on a log-log scale). This is very similar to the behavior observed for the two notches in Test 3.1. The inability of present theory to explain these results points out a need for additional theoretical analysis.



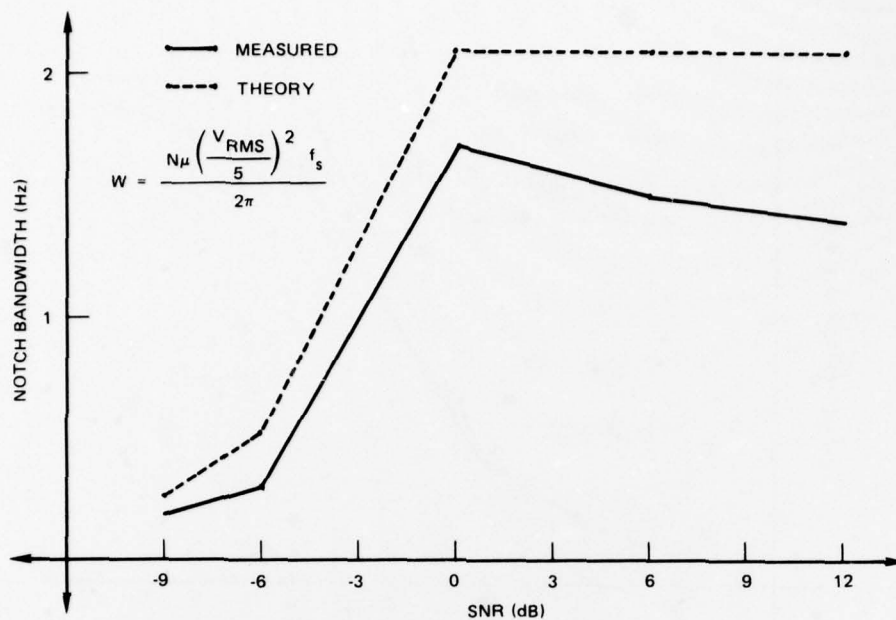


Figure 38. Test 4.2 – plot of notch width versus reference signal-to-noise ratio.

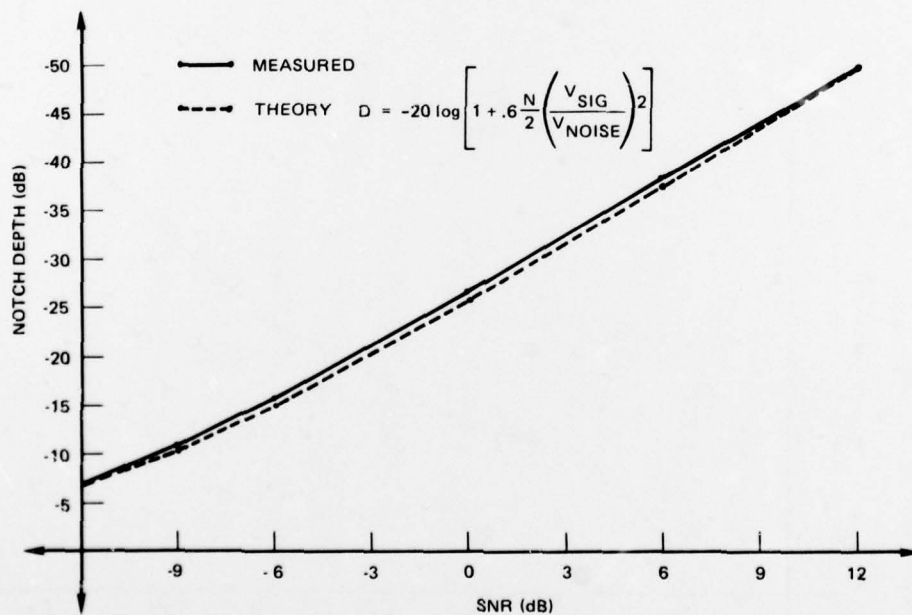


Figure 39. Test 4.2 – plot of notch depth versus reference signal-to-noise ratio.

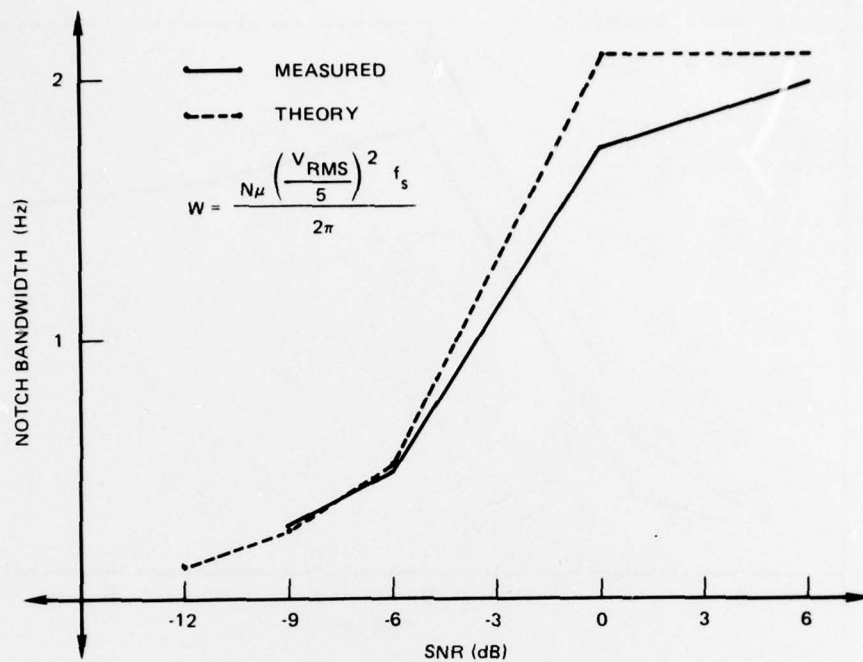


Figure 40. Test 4.3 – plot of notch width versus reference signal-to-noise ratio.

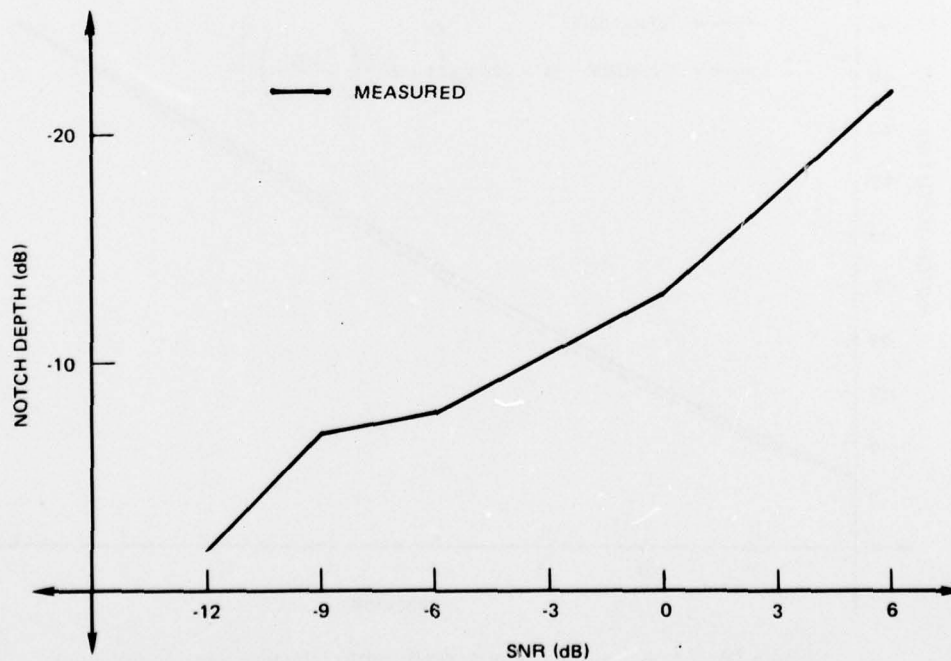


Figure 41. Test 4.3 – plot of notch depth versus reference signal-to-noise ratio.

## APPENDIX A

Discussed here, are some of the interrelations between equations (1) through (3) and the actual experimental setup. The internal scaling of the ANC box (see fig 1) results in the relationships

$$\hat{\mu} \sigma^2 = \frac{\mu}{2} \left( \frac{V_{RMS}}{5} \right)^2 \quad (A-1)$$

where  $\hat{\mu}$  is the feedback constant in (volt)<sup>-2</sup>,  $\mu$  is the feedback as read on the front panel, and  $\sigma^2$  is the reference power in (volt)<sup>2</sup>.

For a single sinusoid, with the weights initially set at 0, the output will exhibit a single time constant (refs 1, 3, 4) given by the substitution of (A-1) into (1) (with  $\sigma_n^2 = 0$ )

$$\tau = \frac{2}{\mu N \left( \frac{V_{RMS}}{5} \right)^2 f_s} \quad (A-2)$$

Note, that the sample rate  $f_s$ , is included to convert from time in number of sample points to time in seconds.

The broadband case is somewhat more difficult. If the spectrum is perfectly white (infinite roll-off at the Nyquist frequency and  $\sigma_s^2 = 0$ ) the formula

$$\tau = \frac{1}{\mu \left( \frac{V_{RMS}}{5} \right)^2 f_s} \quad (A-3)$$

holds. A more general formula for the smallest time constant which holds even when the spectrum is not flat is given by (ref 4)

$$\tau = \min_{\omega} \frac{1}{2\hat{\mu} S(\omega) f_s} \quad (A-4)$$

where  $S(\omega)$  is the spectral level of an N point FFT of the reference input.

More precisely,

$$S(m) = \sum_{\ell=1}^N R(\ell) e^{i\ell M/N},$$

$$= \frac{N}{2} \frac{\text{power}}{\text{cell}}.$$
(A-5)

For broadband inputs, (A-5) may be rewritten,

$$S(m) = \frac{\text{power}}{\text{Hz}} \frac{f_s}{2}.$$
(A-6)

For a broadband signal which consists of white noise, which has been bandpass filtered at bandwidth  $B$ , the power/Hz of the spectrum is given by  $\sigma_n^2/B$ . For a sinusoid, the power/cell is  $\sigma_s^2$ . Thus, (A-4) to (A-6) yielded,

$$\max_m S(m) = \frac{N}{2} \sigma_s^2 + \frac{\sigma_n^2}{B} \frac{f_s}{2},$$
(A-7)

$$\tau = \frac{1}{2\mu \left( \frac{N}{2} \sigma_s^2 + \sigma_n^2 \frac{f_s}{2B} \right) f_s}.$$
(A-8)

Equation (A-8) is more general than (1), and reduces to (1) when the noise is white, i.e., its bandwidth is the Nyquist frequency  $f_s/2$ .

When only the sinusoid is present, (A-8) gives (A-2); however, for broadband noise, (A-3) must be replaced by

$$\tau = \frac{1}{\mu \left( \frac{V_{RMS}}{5} \right)^2 f_s} \frac{B}{f_s}$$
(A-9)

(derived by substituting (A-1) and (A-8) and setting  $\sigma_s^2 = 0$ ).

In the present experiments, the noise was low pass filtered at 600 Hz (3 dB down-point). Since  $f_s = 2048$ ,  $2B = .6 f_s$ , and the appropriate formula is,

$$\tau = \frac{.6}{\mu \left( \frac{V_{RMS}}{5} \right)^2 f_s}.$$
(A-10)



Strictly speaking, several time constants will be present and the regions of the output spectrum beyond 600 Hz converge more slowly (ref 4). An example of this appears in figure A-1. Even after 10 time constants, the higher frequencies (above 750 Hz) have not converged.

In order to measure the single time constant given by equation (A-11), the slower modes were filtered out by including a post-filter identical to the prefilter (fig 2). Also, as a test of the above theory, test 1.1 was rerun with the filter set at 1000 Hz, giving a roll-off of 3 dB at 860 Hz and compared with the theoretical formula

$$\tau = \frac{.86}{\mu \left( \frac{V_{RMS}}{5} \right)^2 f_s}; \quad f_s = 2^{11}. \quad (A-12)$$

The results are plotted in figure A-2 and, just as in figure 5, show excellent agreement.

Finally, we wish to remark that the above time constants were measured with respect to amplitude; i.e., volts RMS; and hence are twice as large as they would be for the output power. The experimental values were determined by fitting a curve of the form  $Ae^{-t/\tau} + A_0$  to the data.

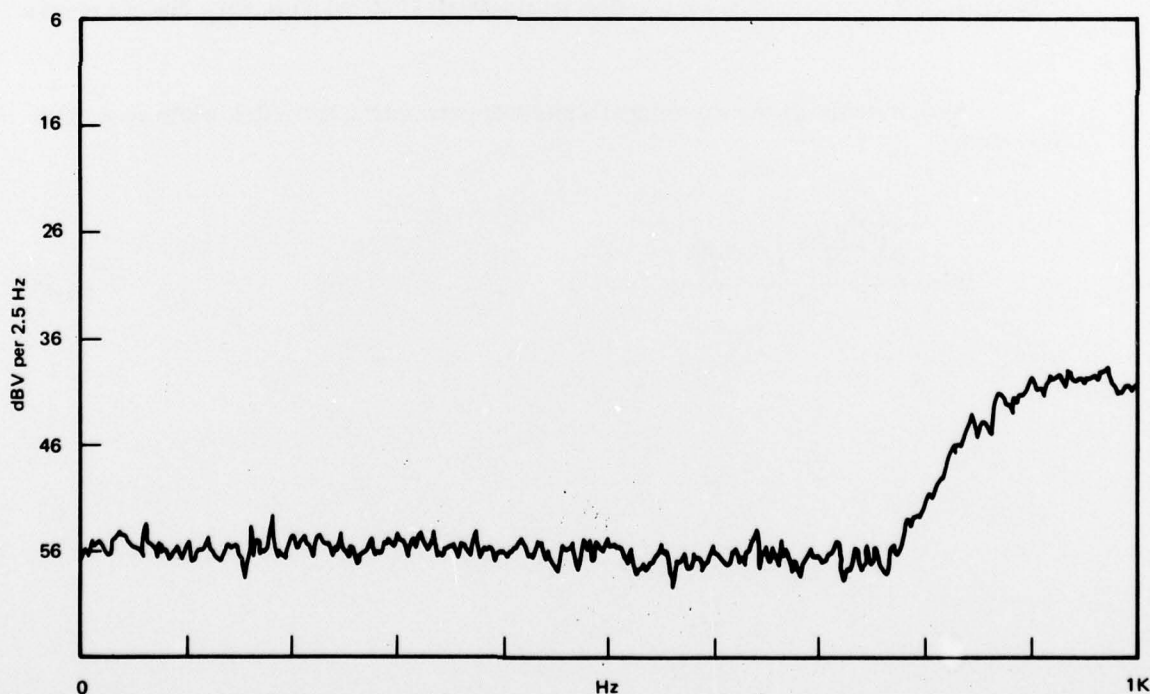


Figure A-1. Output of ANC with no post-filter after about 10 time constants. The roll-off of the prefilter was 3 dB at 600 Hz.

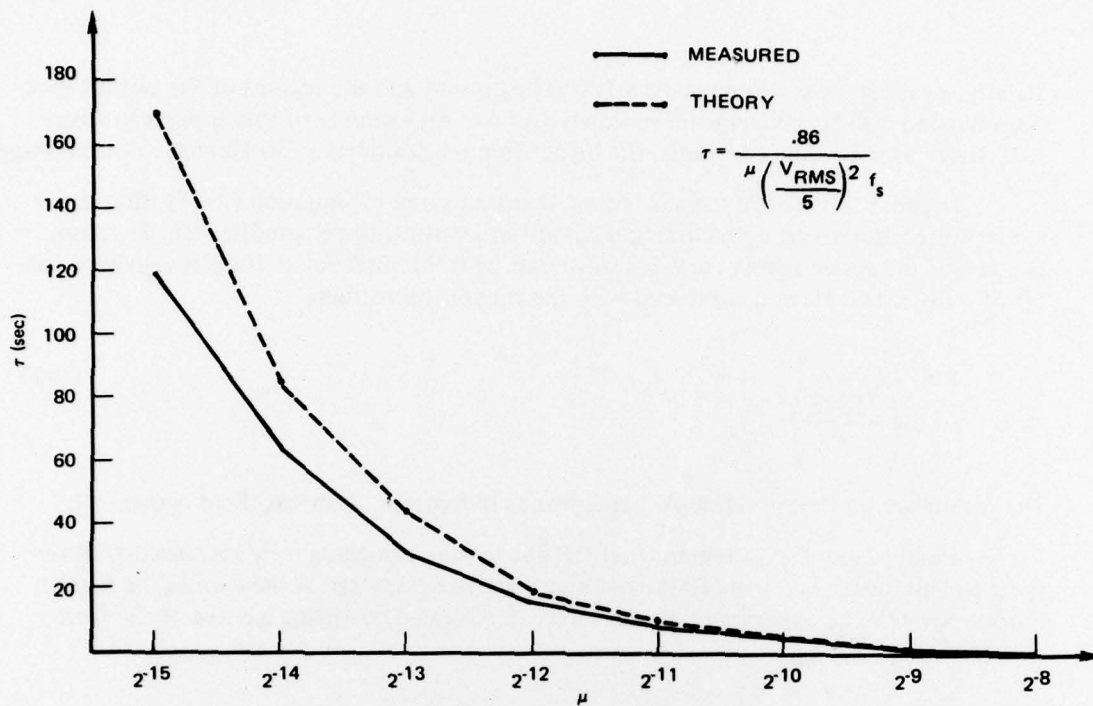


Figure A-2. Test 4.1 with prefilter and post-filter set at 1000 Hz (3 dB roll-off at .86) – Plot of  $\tau$  versus  $\mu$ .

Also, in terms of the experiment's physical parameters, the notch width (e.g., (2)) is given by

$$W = \frac{\mu \left( \frac{V_{RMS}}{5} \right)^2 f_s N}{2\pi} \quad (A-13)$$

## APPENDIX B – MEASUREMENT OF $\tau$ IN TEST 3.1

Although we have been fitting exponentials to the learning curves, it is more convenient here to use the more exact formula (ref 4),

$$\text{output} = A(1 - 1/f_s\tau)^n. \quad (\text{B-1})$$

Then,

$$\begin{aligned} 20 \log(\text{output}) &= 20 \log A - n/f_s\tau \text{ where } f_s\tau \gg 1 \\ &= 20 \log A - t/\tau. \end{aligned} \quad (\text{B-2})$$

Then, by converting the logarithms to the base 10

$$\text{slope of output (dB)} = -\frac{20}{\log 10} \frac{1}{\tau}. \quad (\text{B-3})$$

When more than two time constants are present, the above technique is usually valid provided the time constants are widely separated and the curve is straight over a range of about 6 dB. This may be seen as follows.

Approximate the curve by:

$$A(1 - \lambda)^n + B, \quad (\text{B-4})$$

where the faster time constants have died out and the slower ones are almost constant (i.e.,  $= B$ ). The logarithmic slope of (B-4) is given by,

$$\frac{1}{n(1 - \lambda)^n + B} nA(1 - \lambda)^{n-1} = \frac{n}{(1 - \lambda) + \frac{B(1 - \lambda)}{nA(1 - \lambda)^n}}. \quad (\text{B-5})$$

The second term in the denominator will be negligible, provided  $B < A(1 - \lambda)^n$ ; i.e., provided the magnitude of the function in (B-4) is at least 6 dB larger than B. See figure 30 for an example.

## APPENDIX C

<u>QUANTITY</u>	<u>EQUIPMENT USED</u> <u>TYPE</u>
1	Universal Adaptive Filter, Rockwell/Autonetics Mod 3
1	Spectrum Analyzer, Nicolet Scientific Mini-Ubiquitous Model 444A
1	Spectrum Analyzer, Nicolet Scientific Mini-Ubiquitous Model 440A
1	Digital Signal Processor, Spectral Dynamics Model SD 360
1	Frequency Translator, Nicolet Scientific Model 30A/LIS
1	Frequency Translator (Master) Spectral Dynamics Model SD 332
1	Frequency Translator (Slave) Spectral Dynamics Model SD 332-2
1	Interactive Digital Plotter, Tektronics Model 4662
1	X-Y Plotter with Time Drive, Hewlett-Packard Model HP 7004A
1	X-Y Plotter, MFE Model 715
1	Pseudo-Random Sequence Generator, Hewlett-Packard Model HP01-3722A
1	Random Noise Generator, General Radio, Model GR 1381
2	Frequency Synthesizer, Fluke Model 6010A
1	Frequency Synthesizer, Rockland Model 5100
1	Frequency Synthesizer, Wavetek Model 171
1	Strip Chart Recorder, Gultan Model TR 222
1	True RMS Voltmeter, Hewlett-Packard Model HP 3403C
1	Pulse Generator, Data Pulse Model 101
1	High Resolution Counter, Hewlett-Packard Model HP 5307A
3	Filter, Krohn-Hite Model 3202
1	Attenuator Set, Hewlett-Packard Model 350B
2	Attenuator Set, NOSC Manufactured
2	Summing Amplifier, NOSC Manufactured
2	Impedance Converter, NOSC Manufactured